A Spiking Neuron Model: Applications and Learning

Chris Christodoulou[a, b, 1], Guido Bugmann[c] and Trevor G. Clarkson[b, d]

[a]*School of Computer Science and Information Systems*
Birkbeck College, University of London, Malet Street, London WC1E 7HX, UK
[b]*Department of Electronic Engineering, King's College, University of London, Strand, London WC2R 2LS, UK*
[c]*School of Computing, University of Plymouth, Plymouth PL4 8AA, UK*
[d]*Engineering & Research, 9G/6D, Radiocommunications Agency*
Wyndham House, 189 Marsh Wall, London E14 9SX, UK

Abstract

This paper presents a biologically-inspired, hardware-realisable spiking neuron model, which we call the Temporal Noisy-Leaky Integrator (TNLI). The dynamic applications of the model as well as its applications in Computational Neuroscience are demonstrated and a learning algorithm based on postsynaptic delays is proposed. The TNLI incorporates temporal dynamics at the neuron level by modelling both the temporal summation of dendritic postsynaptic currents which have controlled delay and duration and the decay of the somatic potential due to its membrane leak. Moreover, the TNLI models the stochastic neurotransmitter release by real neuron synapses (with probabilistic RAMs at each input) and the firing times including the refractory period and action potential repolarisation. The temporal features of the TNLI make it suitable for use in dynamic time-dependent tasks like its application as a motion and velocity detector system presented in this paper. This is done by modelling the experimental velocity selectivity curve of the motion sensitive H1 neuron of the visual system of the fly. This application of the TNLI indicates its potential applications in artificial vision systems for robots. It is also demonstrated that Hebbian-based learning can be applied in the TNLI for postsynaptic delay training based on coincidence detection, in such a way that an arbitrary temporal pattern can be detected and recognised. The paper also demonstrates that the TNLI can be used to control the firing variability through inhibition; with 80% inhibition to concurrent excitation, firing at high rates is nearly consistent with a Poisson-type firing variability observed in cortical neurons. It is also shown with the TNLI, that the gain of the neuron (slope of its transfer function) can be controlled by the balance between inhibition and excitation, the gain being a decreasing function of the proportion of inhibitory inputs. Finally, in the case of perfect balance between inhibition and excitation, i.e., where the average input current is zero, the neuron can still fire as a result of membrane potential fluctuations. The firing rate is then determined by the average input firing rate. Overall this work illustrates how a hardware-realisable neuron model can capitalise on the unique computational capabilities of biological neurons.

---

[1] Corresponding Author. Tel.: +44 20 7631 6718; fax: +44 20 7631 6727; Email: chris@dcs.bbk.ac.uk

1. Introduction

There are several types of spiking neuron models ranging from detailed biophysical ones to the `integrate-and-fire` type (for an excellent review, see Gerstner, 1998) which form the basis of spiking neuron networks (Maass, 2001). A class of the more detailed models, known as conductance-based ones, have their origins in the classic work by Hodgkin & Huxley (1952) (H&H) who have summarised their experimental studies of the giant axon of the squid in four differential equations. The main equation describes the conservation of electric charge on a piece of membrane capacitance of a neuron under the influence of a current and a voltage (see Cronin, 1987, for a detailed mathematical analysis). The H&H equations can be regarded as describing the variations of membrane potential and ion conductances that occur `naturally` at a fixed point on the axon. Due to the model's success there have been several attempts to generalise it in order to describe other experimental situations (see for example Jack *et al.*, 1975, for a review). Although this model has originally been designed to describe the form of a temporal change of an action potential during axonal transmission, analogous models to the H&H equations which include additional ion channels, have been recently used to describe spike generation at the soma of the neuron (Bernander *et al.*, 1991; Bush & Douglas, 1991; Ekeberg *et al.*, 1991; Rapp *et al.*, 1992; Stuart & Sakmann, 1994). Due to the complexity of the H&H equations, mainly caused by their nonlinearity and four-dimensionality, various simpler models have been proposed; FitzHugh (1961) and Nagumo *et al.* (1962) and more recently Abbott & Kepler (1990) systematically reduced the H&H equations to two variables, so as to allow a phase plane analysis of a stationary and oscillatory states of the system (Rinzel & Ermentrout, 1998).

A different approach takes the neuron as a leaky integrator which is *reset*, if firing occurs. This leads to the class of *leaky integrate-and-fire* (LIF) models which have been studied extensively by Stein (1967). The LIF model was first employed by Lapicque (1907) (see Tuckwell, 1988 for a detailed description of the *Lapicque model*). This model is a very simple mechanism of spike generation and dendritic integration. A detailed discussion of the properties of the LIF model for different sets of parameters is given in Stein (1967) and Jack *et al.*, (1975). The LIF model gives in general a simple picture of neuronal spike generation which is primarily based on the loading time of the cell. Abbott & Kepler (1990) have shown that the more complex H&H model can be reduced to an LIF model in the limit that the membrane loading time is the dominant time scale of the neuronal dynamics.

In order to examine the temporal capabilities of biological neurons one needs to incorporate in modelling more of the details of neuronal structure. One should consider for example the relative effectiveness of the synapses close to the soma compared to those of the same strength on distal parts of the dendritic tree or consider how branching affects the integration of various inputs. These and other issues that mainly deal with the cell geometry and in particular with *passive nerve cylinders* (i.e., ones for which the membrane conductance is fixed) or *cables* can be described by *partial differential equations* of *linear cable theory* which can represent the entire dendritic tree (Hodgkin & Rushton, 1946; Davis & Lorente de Nó, 1947; Rall, 1959; 1962; 1977; Jack *et al.*, 1975; see also Rall & Agmon-Snir, 1998 for a recent review). With cable theory one can get straightforward analytical solutions for transient current inputs to an idealised class of dendritic trees that are equivalent to unbranched cylinders (Rall, 1959). However, for nonuniform dendritic trees with general branching structure (Butz & Cowan, 1974; Horwitz, 1981;1983; Wilson, 1984; Koch & Poggio, 1985) and for spatiotemporal inputs associated with synaptic current produced by conductance changes (Rinzel & Rall, 1974; Poggio & Torre, 1977;

Koch *et al.*, 1982; Holmes, 1986), the solutions become much more complicated. In such cases, it is simpler and less computationally expensive to use *compartmental models* rather than analytical models (Rall, 1964; see also Segev & Burke, 1998 for a review). The main advantage of the compartmental approach over cable theory is flexibility. Firstly, the membrane properties and the amount of synaptic conductance input or current injection can be different in every compartment and secondly dendritic branching may not need to satisfy equivalent-cylinder constraints. It is also possible with compartmental models to compute the consequences of any branching geometry and any possible input spatiotemporal pattern (Bressloff & Taylor, 1993). In case of complex models the compartmental approach leads to simpler and less computationally expensive treatment of dendritic structure than cable theory and has been used extensively in computational studies of neuronal systems (Koch & Segev, 1998).

All the above models include the important characteristics of *nonlinearity* (caused for example by the action potential generation mechanism) and some of them incorporate *temporal sensitivity* (arising from the *dendritic geometric structure,* from *leaky membranes* and the time course of numerous ionic currents).

However, few of them include *intrinsic stochasticity* which is another very significant characteristic of real neurons. Neurophysiological evidence (Katz, 1969; Pun *et al.*, 1986; Redman, 1990), indicates that there is a large number of synapses with a small probability to release a quanta of neurotransmitter, i.e., an input spike does not always produce a postsynaptic potential (excitatory or inhibitory). The probability distribution of quantal release is determined in general by a Bernoulli (1 vesicle), binomial (many vesicle) or compound binomial distributions occurring on arrival of a nerve impulse; similar although lower probability distributions occur as part of the spontaneous activity on the cell body, when there is no nerve impulse (Taylor, 1972). The importance of noise in models was, for instance, pointed out by Buchmann & Schulten (1987) who showed, by including a noise source to the membrane potential dynamics, that the membrane potential fluctuations induce spontaneous spike activity and that noise regulates the level of attention, possibly comparable to the arousal level in animals.

In Section 2 of this paper we present a spiking neuron model, the Temporal Noisy-Leaky Integrator (TNLI) incorporating the important features of single cells identified above, i.e., of nonlinearity, temporal sensitivity and intrinsic stochasticity as well as being hardware realisable. Section 3 demonstrates how the TNLI can be used as a motion and velocity detector system. This is done by modelling the experimental velocity selectivity curve of the motion sensitive H1 neuron of the visual system of the fly as measured by Franceschini (Franceschini, 1985; Franceschini *et al.*, 1989). Section 4 starts by referring to experimental and modelling work on synaptic plasticity and then describes a Hebbian-based learning technique which enables the TNLI to be successfully trained to detect an arbitrary temporal pattern. The work presented in Sections 3 and 4 is an extension of the preliminary results presented in Christodoulou *et al.* (1992; 1995) respectively. Section 5 discusses extensively the role of stochastic synapses (1-pRAMs) in the TNLI. Sections 6 and 7 describe applications of the TNLI in Computational Neuroscience: the first identifies inhibition as one of the determinants of the highly variable firing observed in neurons and demonstrates how it can be used to control it and the latter shows how the TNLI can be used to control the gain of the neuron through inhibition. A preliminary report on the latter has been presented in Christodoulou *et al.* (2000). The paper finishes with a discussion in Section 8.

2. The Spiking Neuron model: Temporal Noisy-Leaky Integrator

The TNLI neuron model (Christodoulou *et al.*, 1992), is a simple, biologically inspired and hardware realisable computational model. Fig. 1 shows an analogue hardware outline of the TNLI using a pRAM (probabilistic RAM, Clarkson *et al.*, 1992; 1993) at each input and a Hodgkin & Huxley (1952) equivalent circuit for a leaky cell membrane. Details of how the TNLI can be realised in digital hardware can be found in Christodoulou *et al.* (1992); they are not given in this paper since all the results presented here are taken through software simulations of the TNLI.
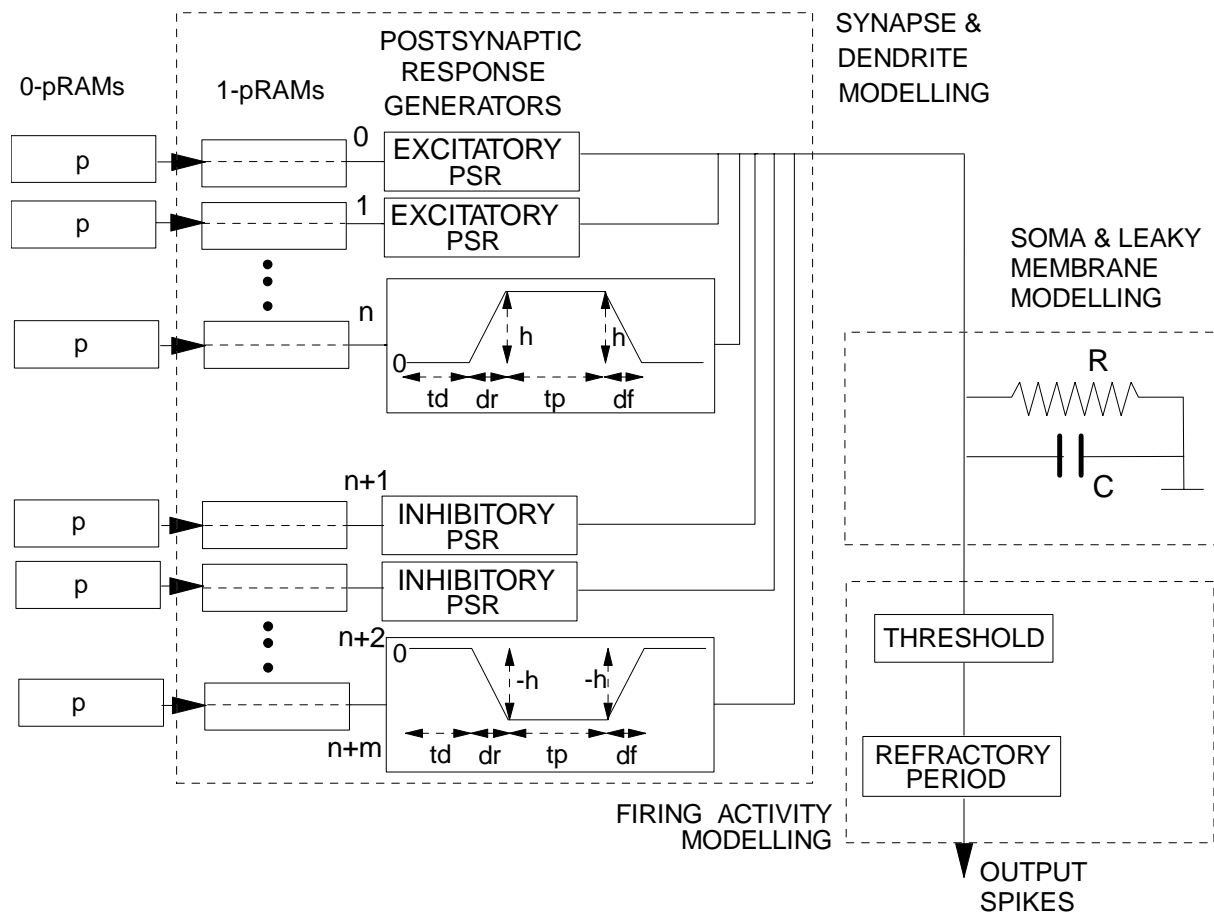

Figure 1: Analogue hardware outline of the TNLI neuron model. The dotted line boxes indicate the corresponding parts of the real neuron which the TNLI modules are inspired by. At inputs n and $n + m$, the Postsynaptic Current Response shapes utilised are shown (EPSCs and IPSCs respectively) where: t_d: Synaptic delay time, t_p: Peak Period time, d_r: Rise time, d_f: Fall time, h: Postsynaptic Peak Current.

2.1 Synaptic and dendritic modelling

The 1-pRAMs in the TNLI model the stochastic and spontaneous neurotransmitter release by the synapses of real neurons, i.e., stochastic synapses can either generate EPSPs (Excitatory Postsynaptic Potentials) spontaneously or cause presynaptic spikes to fail to produce EPSPs. The 0-pRAMs shown in the model (Fig. 1) are used in the simulations to produce random spike input trains from other neurons of controlled mean input frequency, according to their probability p. The postsynaptic response (PSR) generators (Fig. 1), model the effects of dendritic propagation of the postsynaptic potentials and in particular their *temporal summation* (Nicholls *et al.*, 1992).

The presynaptic transmitter release creates an ion-specific conductance change in the postsynaptic neuron which in the TNLI we approximate with an inward or outward current flow model (see eqn. 2, Section 2.3). The separation of dendritic and somatic integration make the current-based model approximation necessary, because a current input is needed to the leaky integrator circuit following in the model, which is the *active* single-compartment representing the somatic membrane. We have therefore voltage as output of that circuit, representing the somatic membrane potential. For every spike generated by the pRAMs, the PSR generators produce postsynaptic current responses $PSR_{ij}(t)$ (i.e., a postsynaptic response at neuron *i* caused by an input spike at time *t* from input neuron *j*), of controlled shapes, shown in Fig. 1 (at inputs *n* and *n* + *m*), which can either be excitatory (Excitatory Postsynaptic Currents, EPSCs) or inhibitory (Inhibitory Postsynaptic Currents, IPSCs). Such EPSCs and IPSCs extended in time, have been used previously in the form of an alpha function (see Walmsley & Stuklis, 1989 and references therein). In the TNLI, these particular ramp shapes chosen for the PSRs are an approximation of alpha functions in the form of linear splines that can easily be implemented in digital hardware.

2.2 Modelling of the soma, the somatic membrane and the firing times

The EPSCs and IPSCs are then summed temporally and the total postsynaptic current response is fed into the RC circuit (Fig. 1). The synaptic saturation that occurs in the real neuron during the temporal summation of the postsynaptic potentials (Burke & Rudomin, 1977) is not currently modelled in the TNLI, but it could be easily incorporated by applying the methods used in (Bugmann, 1992). The capacitance *C* and the resistance *R* represent the somatic leaky membrane of real neurons and therefore this circuit models the decay that occurs in the somatic potential of the real neuron due to its membrane leak. The capacitance *C* and the resistance *R* are fixed at a suitable value to give the leaky membrane time constant ($\tau = RC$). For simplicity, the TNLI does not differentiate in its leaky integrator circuit between different ionic currents as may occur in the real neuron. If the potential of the capacitor exceeds a constant threshold (V_{th}), then the TNLI neuron fires. It then waits for an absolute refractory period (t_R) and fires again if the membrane potential is above the threshold after the refractory period elapses. Therefore, the maximum firing rate of the TNLI is given by $1/t_R$. In this model the integration of inputs continues during the refractory time, but without having the value of the membrane potential compared with the firing threshold during that time. Depending on the application for which the TNLI is being used, the membrane potential, i.e., the potential of the capacitor, can be completely discharged or *reset* whenever the neuron fires (Christodoulou & Bugmann, 2000) (as in Lapique, 1907) or not reset at all (Christodoulou *et al.*, 1992) (as in Bressloff & Taylor, 1991) or partially reset (as in Bugmann *et al.*, 1997).

2.3 Theoretical basis of the TNLI

Most of the leaky integrator models are based on the equation that Hodgkin & Huxley (1952) used to describe the generation of an action potential in the giant squid axon (a similar equation was first used by Lapique, 1907). By linearising that equation, a simplified version for a network of single-compartment leaky integrator neurons with synaptic noise (as used in Bressloff & Taylor, 1991), can be described by the shunting differential equation:

$$C_i \frac{dV_i}{dt} = -\frac{V_i(t)}{R_i} + \sum_{j \neq i} \Delta g_{ij}(t) \times [S_{ij} - V_i(t)] \tag{1}$$

where the term on the LHS is the variation of accumulated charge in neuron i, the first term on the RHS the the membrane leakage current in neuron i (negative term) and the second term on the RHS is the synaptic input current which is excitatory for $S_{ij} > 0$ and inhibitory for $S_{ij} < 0$ (where 0mV is considered to be the resting membrane potential instead of -70mV).

$V_i(t)$ is the membrane potential of the ith neuron at time t and Δg_{ij} is the increase in conductance at the synaptic connection between neuron j and neuron i, with membrane reversal potential S_{ij}, due to the release of chemical neurotransmitters. R_i is the leakage resistance and C_i the somatic capacitance of the membrane.

The TNLI corresponds to the model described by eqn. 1 since it consists of a single active compartment representing the soma and performing integration of EPSCs and IPSCs. For the hardware TNLI model however, eqn. 1 is further simplified by assuming that $S_{ij} \gg V_i(t)$ for excitatory synapses and $S_{ij} \ll V_i(t)$ for inhibitory synapses. Then $[S_{ij} - V_i(t)]$ in term (III) of eqn. 1 can be approximated as S_{ij}, so the synaptic current flow is independent of the membrane potential. With this independence assumption, the shunting effects of the conductance are removed. Note that for our simulations, the resting membrane potential is shifted to 0mV for simplicity. Term *(III)* as a whole, which represents the current flow into the soma, corresponds in our model to the total postsynaptic response current produced by the temporal summation of the postsynaptic current responses each of which is initiated by an input spike. Thus, after the above approximation, the leaky integrator equation for the TNLI becomes:

$$C_i \frac{dV_i}{dt} = - \frac{V_i(t)}{R_i} + \sum_j \sum_{0 \le t_k \le T} PSR_{ij}(t - t_k) \qquad (2)$$

where $PSR_{ij}(t-t_k)$ is the postsynaptic current response caused by an input spike having arrived at time t_k from input neuron j. The response can either be excitatory or inhibitory depending on the sign of PSR_{ij}. T is the total number of time steps that the system is left to operate. Discrete time steps are used in the simulations so dt can be replaced by Δt in eqn. 2, and the double summation term represents current so we can call it $I(t)$. In the hardware model of the TNLI neuron (Christodoulou *et al.*, 1992) the postsynaptic current responses are temporally summed in a counter where they are multiplied at regular time intervals with a decay rate. The term $C_i \Delta V_i$ (which results after discretisation) represents the counter contents in the TNLI and can be written as $C_i V_i(t+\Delta t) - C_i V_i(t)$. So with the above simplifications, eqn. 2 becomes (after dropping the i notation):

$$CV(t+\Delta t) = CV(t) + I(t) \times \Delta t - \frac{V(t)}{R} \Delta t \qquad (3)$$

In the hardware model of the TNLI this equation can be realised in two steps:
First step:

$$CV^*(t) = CV(t)_{before} + I(t) \times \Delta t \qquad (4)$$

and the second step:

$$CV(t+\Delta t) = \alpha \times CV^{*}(t) \, , \qquad \alpha < 1 \tag{5}$$

where α is the decay rate with which the initial counter output contents ($CV^{*}(t)$) are multiplied before they are routed back to the counter via the load input. In other words this decay rate replaces the term $[(-V(t)/R_i) \times \Delta t]$ due to the hardware structure. The relationship between the decay rate α and the time constant $\tau = RC$ can be deduced from eqns. 3, 4 and 5 and is given by:

$$\alpha = 1 - \frac{1}{RC}\Delta t \tag{6}$$

From eqns. 4 and 5 we deduce that the capacitor is charged according to the equation:

$$V(t+\Delta t) = \alpha \times [V(t) + \frac{I(t) \times \Delta t}{C}] \tag{7}$$

When reset is applied to the TNLI, after each firing at time t, $V(t + \Delta t) \to 0$ (i.e., the membrane potential resets to 0). In other words, the potential of the capacitor (soma) is reset, but the temporal summation of the postsynaptic currents on each input line is not reset. When partial reset is applied to the soma (Bugmann *et al*., 1997) then after each firing at time t, $V(t + \Delta t) \to \beta \times V(t)$; β is the reset parameter taking values between *0* and *1*.

The firing times in the TNLI neuron i (T_n^{i}) are determined (as in Bressloff & Taylor, 1991) by the iterative threshold condition:

$$T_n^{i} = \inf\{t | V_i(t) \geq V_{th_i} \, ; \, t \geq T_{n-1}^{i} + t_R\} \qquad n \geq 1 \tag{8}$$

where V_{th_i} is the threshold voltage of neuron i and n is the time of firing and *inf* means a union satisfying both terms in the brackets.

3. Dynamic Time-Dependent Applications of the TNLI: Motion Detection

In this section we explore the temporal powers of the TNLI given the temporal features of neurons that it incorporates, namely: the dendritic temporal summation (see Section 2.1) and the modelling of the decay of the somatic potential due to its membrane leak, with the leaky integrator circuit (see Section 2.2). The inclusion of the postsynaptic response currents with certain delays and durations (see Section 2.1) was inspired by the results of Reiss & Taylor (1991). These authors showed that neurons with delayed responses of certain duration (reminiscent of the response of retinal ganglion cells to short light pulses, Levick & Zacks, 1970) can be used to store and replay temporal sequences of input patterns. As pointed out in Section 2.1, in the TNLI we have included the temporal function as a property of spike propagation in the postsynaptic dendrites (as observed in motor neurons, Redman, 1986), rather than as a property of the output of the neuron, in addition to the temporality provided by the modelled time course of the somatic potential due to its membrane leak. This allows single neurons, like the TNLI, to exhibit much more complex temporal properties and are indeed well suited for applications of temporal storage. Other potential application fields are the recognition of temporal sequences or the more complex computing in the temporal domain where intensities

are not coded by spike frequencies but by the spike arrival time (Burgi & Pun, 1991). Here we show how motion detection, which is a basic example of temporal sequence recognition, can be performed with the TNLI, while it is an impossible task for formal neurons (e.g., McCulloch & Pitts, 1943; Hopfield, 1984).

3.1 The TNLI as a motion detector

The TNLI performs motion detection in a manner similar to that occurring in the compound eyes of the fly, where visual orientation and course stabilisation rely essentially on the evaluation of the retinal motion patterns perceived by the animal during flight (Hausen & Egelhaaf, 1989; Borst & Egelhaaf, 1995). One of the best characterised biological motion sensitive neurons is the H1 cell of the fly which displays unique response properties. This neuron is sensitive to directional motion, which arises from the pooling of signals from smallfield units, the *correlation* type Elementary Movement Detectors (EMDs, see Hassenstein & Reichardt, 1956; Reichardt, 1961; 1987; Buchner, 1976; 1984). According to observations by Franceschini (1985) and Franceschini *et al.*(1989), the response of the H1 neuron to sequential stimulation of two of its receptor cells occurs after the second light flash is *facilitated* by the first flash (effectively one of the signals is delayed by low-pass filtering). The time span over which the facilitatory control acts, defines a "temporal window" (given by the velocity selectivity curve) which ultimately sets the limits to the speed range of the motion detector. By analysing signals from the H1 motion sensitive neuron of the fly, Bialek *et al.* (1991) tried to address the problem of signal discrimination by attempting to give an answer on how an organism inverts output spikes in order to reconstruct the two input spike trains and thus discriminate them (see also Rieke *et al.*, 1997). Bialek's work (Bialek *et al.*, 1991) is concerned with the extraction of motion information from the spike trains of the H1 cell; we are concerned with how these spikes are produced initially. Some other models have been proposed for motion detection both for the invertebrate retina (Zanker *et al.*, 1999; Srinivasan *et al.*, 1999) and the vertebrate retina (Koch *et al.*, 1986; Koch & Mathur, 1996). The originality of the model we propose here is that the dendritic propagation delays are used rather than temporal filters which is the case with most of the models above.

For realising a motion detector, a TNLI with two inputs I_1 and I_2 is used (Christodoulou *et al.*, 1992). The motion of a stimulus (for instance an edge of a picture) from I_1 to I_2 is encoded by two spikes, one arriving at input I_1 at time t_1 and the other with a certain delay, at input I_2 at time t_2. The faster the motion, the shorter the delay t_2 - t_1. A motion in the opposite direction would result in a first spike arriving at I_2 and a delayed one at I_1.

In order to make the detector direction selective, we have chosen a temporal response to input I_1 with a long duration and an initial postsynaptic delay (t_d = 10ms), as shown in Fig. 2a. The temporal response to input I_2 is short with no delay (t_d = 0), shown in Fig. 2b. The configuration of the postsynaptic responses for two incoming spikes representing the motion of a stimulus, arriving 50ms apart from each other, is presented in Fig. 2c. Curve (1) (continuous line) corresponds to the case of an input spike arriving at input I_1 at time t_1 = 0ms and curve (2) (dotted line) corresponds to the case of an input spike arriving at input I_2 at time t_2 = 50ms.

As pointed out in section 2.1, the temporal responses are modelled in the TNLI as time dependent currents flowing into the soma represented by a capacitor C in parallel with a leak R. The potential V of the capacitor evolves according to eqn. 2 (or eqn. 7). For this particular simulation of the TNLI, the potential of the soma is *not reset* after each output spike so that only the leak
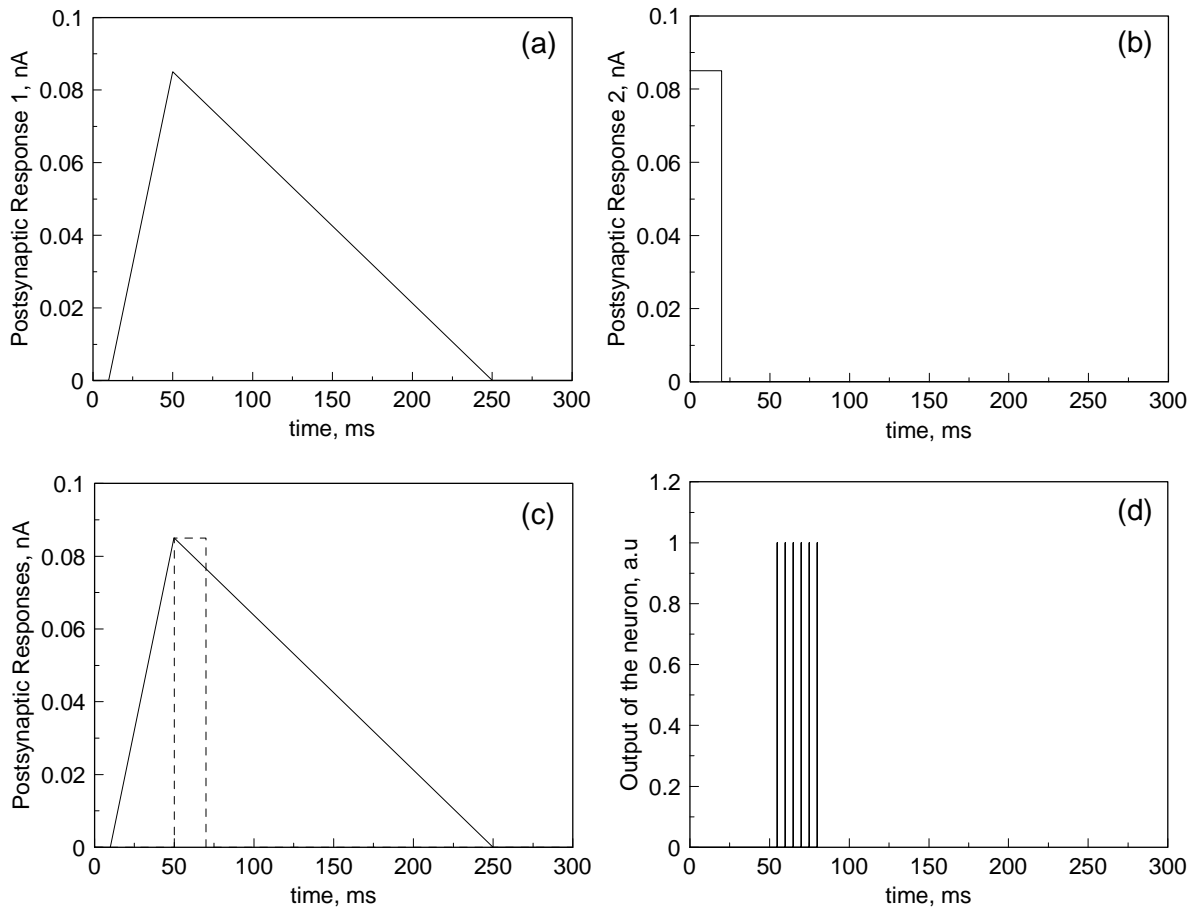
Figure 2: (a), (b) Postsynaptic temporal response functions for: **(a)** input I_1, with a long duration and an initial postsynaptic delay; **(b)** input I_2, with a short duration and no postsynaptic delay. **(c)** Postsynaptic temporal response functions chosen for motion detection: Curve **(1)** (continuous line) corresponding to an input spike arriving at time $t_1 = 0$ms at input I_1 and curve **(2)** (dotted line) corresponding to an input spike arriving at time $t_2 = 50$ms at input I_2. **(d)** Burst of spikes produced by the TNLI neuron for the configuration shown in Fig. 2c.

R can cause a decay of the accumulated charge. Therefore, once the threshold has been reached, the neuron fires in bursts of spikes with frequency limited only by the refractory time. Such a burst is shown in Fig. 2d for the output configuration exemplified in Fig. 2c.

The parameters are chosen as follows: $C = 6 \times 10^{-11}$F, $R = 166$MΩ ($\tau = RC = 10$ms), maximum amplitude of the temporal response function : 0.085nA (this ensures that a single temporal response cannot generate an output, but allows two temporal responses with the correct timings to do so), $t_R = 5$ms. The memory contents α_{01}, α_{11}, α_{02}, α_{12} of the two 1-pRAMs used at the

inputs are set to $\alpha_{0i} = 0$ and $\alpha_{1i} = 1$. In this case, the 1-pRAMs fire for every arriving spike. The 0-pRAMs are not used here.

With the above described temporal response functions and parameters, the motion detector becomes perfectly direction selective, responding only when I_1 is stimulated first. There is no response when a spike arrives at I_2 first. The selectivity to the velocity of the motion depends on the choice of the temporal response function induced by the first arriving spike (Fig. 2a). With a temporal response as in Fig. 2a, the neuron responds to a rather broad range of velocities. This
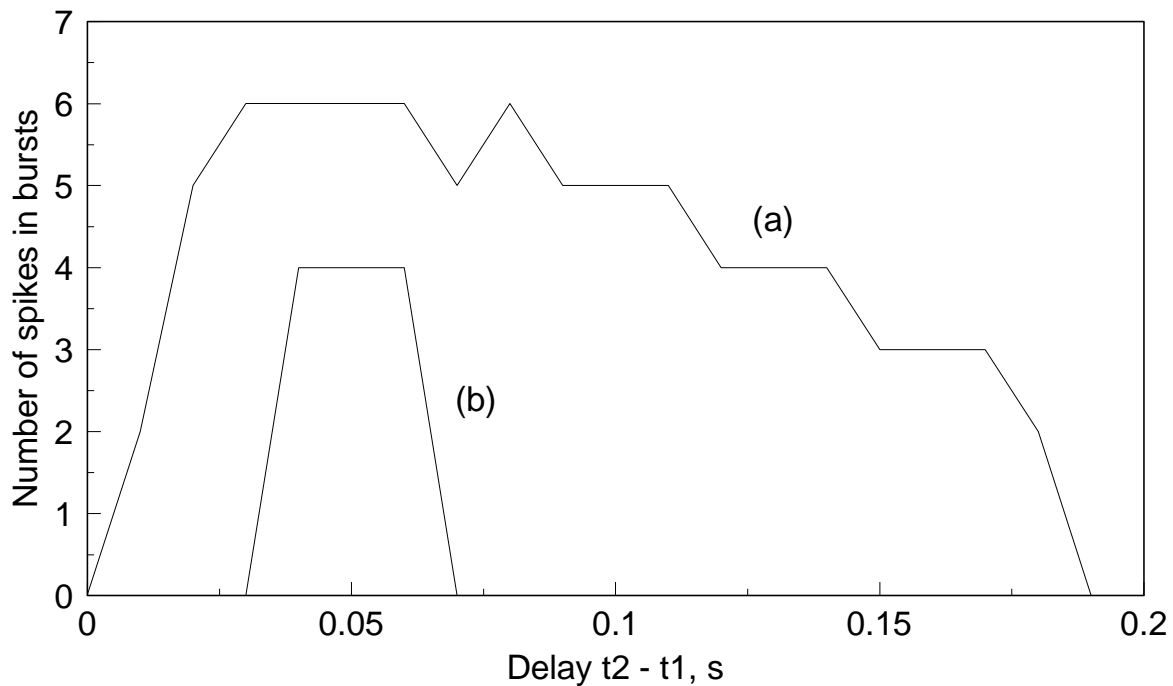
Figure 3: Velocity selectivity of the TNLI neuron used as a motion detector. The velocity is proportional to $1/(t_1 - t_2)$. The curves show the selectivity of the motion: (a) when the first arriving spike induces the temporal response function of Fig. 2a and (b) when an identical short temporal response, as in Fig. 2b, for both inputs is chosen. Curve (a) is very similar to the curve measured experimentally in the motion-sensitive H1 neuron of the visual system of the fly.

is shown in Fig. 3, curve (**a**), where the velocity is proportional to $1/(t_2 - t_1)$. With an identical short temporal response for both inputs (as in Fig. 2b), the neuron becomes much more selective for a certain velocity. This is demonstrated in Fig. 3, curve (**b**), which shows the velocity selectivity of the neuron when an identical short response (as the one in Fig. 2b) for both inputs is used.

We may note that the broad velocity selectivity curve of Fig. 3, curve (**a**), is very similar to the curve measured experimentally in the neuron H1 in the visual system of the fly by Franceschini, (see Fig. 17 in Franceschini, 1985 or Fig. 13 in Franceschini *et al.,*1989). A low-level processing

vision system for a robot, inspired by the visual system of the fly, was successfully demonstrated by Franceschini (Franceschini *et al.*, 1991; 1992), which uses the principle of facilitatory control. We believe therefore that our temporal neuron has also potential applications in artificial vision and could probably readily be incorporated in the system of Franceschini *et al*. (1991; 1992). It has to be pointed out that despite the relative simplicity of the computations underlying the different control systems in the fly visual system and indeed in the TNLI, these systems are fast, reliable and robust against noisy signals.

4. Hebbian-based learning rule for training the postsynaptic delays in the TNLI

From section 3.1 on the motion sensitive neurons in the visual system of the compound eye of the fly, there is no learning going on in the correlation type EMDs. Similarly, in the application of the TNLI as a motion and velocity detector system, no learning was applied to the system. Recent experimental evidence from neurons in the neocortex (Markram *et al.*, 1997) suggests that

synaptic modification depends on the relative timing of a pair of pre- and postsynaptic action potentials and that changes in EPSPs are induced by coincidence of postsynaptic action potentials with unitary EPSPs. Several attempts have been made since then to emulate these results by extending and generalising the Hebbian learning rule (Hebb, 1949) and basing it on spike timing rather that firing rates (Kempter *et al.*, 1999; Song *et al.*, 2000; Kistler & van Hemmen, 2000; Senn *et al.*, 2001a; Kitajima & Hara, 2000; Fusi *et al.*, 2000). For our case, the aim was not to reproduce the results by Markram *et al.* (1997), but to have a simple learning rule for the TNLI, which would modify the postsynaptic current responses accordingly so that any arbitrary repeated temporal pattern would later preferentially be detected and recognised. In other words, we were aiming for a learning rule for artificial systems, which would not necessarily be a good rule in biological systems. We incorporated therefore in the TNLI a simple Hebbian-based learning rule (Christodoulou *et al.*, 1995) aiming to achieve coincidence detection for the PSR currents.

The TNLI fires a spike only if the membrane potential is above the threshold and the neuron is not in the refractory period. It is therefore more convenient to base the training on the membrane potential rather than on the final output (i.e., the occurrence of a spike). In addition, in order to avoid multi-parameter training it is better to choose one of the parameters of the postsynaptic currents to train on. The rule aims at detecting the overlap between two postsynaptic response currents formed by any pair of spikes; if an overlap exists, the rule will increase this overlap by modifying the postsynaptic delays according to the relative difference between the maximum membrane potential at time *t*, $V_{out\_max}(t)$ and the maximum membrane potential at time *t-1*, $V_{out\_max}(t-1)$, where *t* refers to a particular learning trial when a temporal pattern of spikes is presented to the neuron (that is why V_{out_max} is used rather than the singular value of the membrane potential at any point in time). The learning is based on the difference between maximum membrane potential values from two consecutive trials (*t* and *t-1*), rather than the overlap between two postsynaptic responses ($t_{c(mn)}$), since: (i) V_{out_max} is directly proportional to the degree of overlap (a greater $t_{c(mn)}$ leads to a higher V_{out_max}) and (ii) V_{out_max} is directly related to the neuron's output, as pointed out above. In order for the temporal pattern to be detected, the TNLI neuron should fire at any point in time when the pattern passes in front of the neuron's inputs. In other words, the maximum membrane potential should go above the threshold potential in order to enable the desired detection. If different neurons are trained to respond to patterns with different temporal configuration then a dynamic pattern recognition system can be formed.

Whenever two postsynaptic response currents produced by any two spikes of a temporal pattern overlap and the maximum membrane potential produced is below the threshold, then we can modify the relative contribution of the two postsynaptic currents at the given point of reference by modifying the postsynaptic delays to increase the PSR overlap time and consequently increase the membrane potential. For simplicity and for avoiding multi-parameter training, we train only on the postsynaptic delays (t_d) of each input and we keep the area under the PSRs constant. Using a simple Hebbian-based learning for any two spikes coming at inputs *m* and *n* with the first spike arriving at input *m* followed by a spike at input *n* with certain delay T_d, we have, if an overlap exists (i.e., $t_{c(mn)} > 0$):

$$t_{d(m)}(t+1) = t_{d(m)}(t) + \Delta t_{d(m)}(t) \tag{9a}$$

and

$$t_{d(n)}(t+1) = t_{d(n)}(t) - \Delta t_{d(n)}(t) \tag{9b}$$

where $t_{d(m)}(t)$ and $t_{d(n)}(t)$ are the values of the postsynaptic delays at inputs *m* and *n* respectively at time *t* (where time *t* refers to a particular learning trial when the temporal pattern of the two spikes is presented to the neuron). The terms $\Delta t_{d(m)}(t)$ and $\Delta t_{d(n)}(t)$ denote the adjustment applied to the postsynaptic delays at inputs *m* and *n* respectively at trial *t*, and are given by:

$$\Delta t_{d(m)}(t) = \eta \times [V_{out\_max}(t) - V_{out\_max}(t-1)] \times in_m(t) - \alpha \times t_{d(m)}(t) \tag{10a}$$

and

$$\Delta t_{d(n)}(t) = \eta' \times [V_{out\_max}(t) - V_{out\_max}(t-1)] \times in_n(t) - \alpha' \times t_{d(n)}(t) \tag{10b}$$

where η and η' denote the learning rates with $\eta >> \eta'$, α and α' are positive constants with $\alpha >> \alpha'$, since the adjustment applied to the postsynaptic delay at input *n* ($\Delta t_{d(n)}(t)$) should always be extremely small; a large adjustment, might cause the postsynaptic delay at input *n* to become negative, which is wrong, since this will be equivalent to altering the arrival time of the original spike at input *n*, by essentially moving it backwards. The terms $in_m(t)$ and $in_n(t)$ are the input frequencies of the spikes arriving at inputs *m* and *n* respectively at a particular trial *t* (number of spikes per input line divided by the duration of the trial). The second factor of the eqns. 10a and 10b is introduced so as to impose a limit in the exponential growth or reduction and subsequent saturation of the postsynaptic delay (t_d), which would be produced if the first term is used on its own (Kohonen, 1988).

In other words, if there is an overlap between the postsynaptic current responses (i.e., $t_{c(mn)} > 0$), then this overlap time is increased by increasing the postsynaptic delay of the spike arriving first at input *m* (eqn. 9a) and decreasing the postsynaptic delay of the spike arriving second at input *n* (eqn. 9b). If there is no overlap between the postsynaptic response currents (i.e., $t_{c(mn)} = 0$), then no learning is performed.

4.1 Arbitrary single temporal pattern detection and recognition with the TNLI
For testing the above learning rule the TNLI was trained to detect and recognise a temporal pattern consisting of three spikes separated by a certain delay, each arriving at a different input (Christodoulou *et al.*, 1995). For this task only excitatory postsynaptic responses were used. Three inputs only were utilised (I_0 - I_2) and the parameters chosen for the postsynaptic current responses (see Fig. 1) are:
(PSR)$_0$: $d_{r(0)}$ = 5ms, $t_{p(0)}$ = 10ms, $h_{(0)}$ = 60pA, $d_{f(0)}$ = 20ms,
(PSR)$_1$: $d_{r(1)}$ = 5ms, $t_{p(1)}$ = 10ms, $h_{(1)}$ = 60pA, $d_{f(0)}$ = 15ms and
(PSR)$_2$: $d_{r(2)}$ = 5ms, $t_{p(2)}$ = 10ms, $h_{(2)}$ = 60pA, $d_{f(2)}$ = 10ms.

The values chosen for the postsynaptic peak current of each postsynaptic response ensure that one or two responses together cannot generate an output, but allow all three responses with the

correct timings to do so. The three spikes were separated by a delay of T_d = 30ms (as shown in Fig. 5). The postsynaptic delay times which are the trainable parameters, were initially chosen to be: $t_{d(0)}$ = 20ms, $t_{d(1)}$ = 10ms and $t_{d(2)}$ = 5 ms. The rest of the TNLI parameters are: t_R = 5ms, C = 60pF, R = 166MΩ ($\tau = RC$ = 10ms) and V_{th} = 15mV. The simulation time step is 1ms and the pattern is presented to the neuron every 500ms (length of each trial), giving the same input frequency values *in(t)* for all three inputs of 1/500ms = 2Hz. For these simulations, the potential of the capacitor was not reset. The input spikes were unaffected by the 1-pRAM action since the pRAM memory contents were set to `1' for an input spike and `0' for no spike and thus they fired for each input spike.

The learning rates chosen are η = 0.3 and η' = 0.009 and the constants: α = 0.008 and α' = 0.004. Fig. 4 shows how the postsynaptic delays for the three input spikes are modified during training and the variation of the difference between the threshold potential (V_{th}) and the maximum membrane potential expressed as: *error* = V_{th} - V_{max}. The final values of the delays which enable the neuron to detect the pattern in the example of Fig. 4 are: $t_{d(0)}$ = 98ms, $t_{d(1)}$ = 46ms and $t_{d(2)}$ = 41ms. In this example (where more than two spikes represent a temporal pattern), for the optimal detection of the pattern, the PSRs should be shifted to the right; the second term of eqn. 10b is greater for $t_{d(2)}$ than the first term resulting in a negative adjustment which becomes positive when substituted in eqn. 9b, causing $t_{d(2)}$ to increase. For delay $t_{d(1)}$ which undergoes a positive and a negative adjustment since it refers to the PSR in the middle (i.e., (PSR)$_1$, produced after the 2nd arriving spike), the positive adjustment is simply greater than the negative adjustment. That is why in the example all the postsynaptic delays are increased. The learning used is governed by eqns. 9 (i.e., based on the difference between V_{out_max} between two trials), but the *error* is utilised here for demonstration purposes since it gives a measure of the length of the training; the neuron fires and in other words detects the pattern, when the *error* becomes negative. As it can be seen from the example of Fig. 4, the neuron learns to detect the
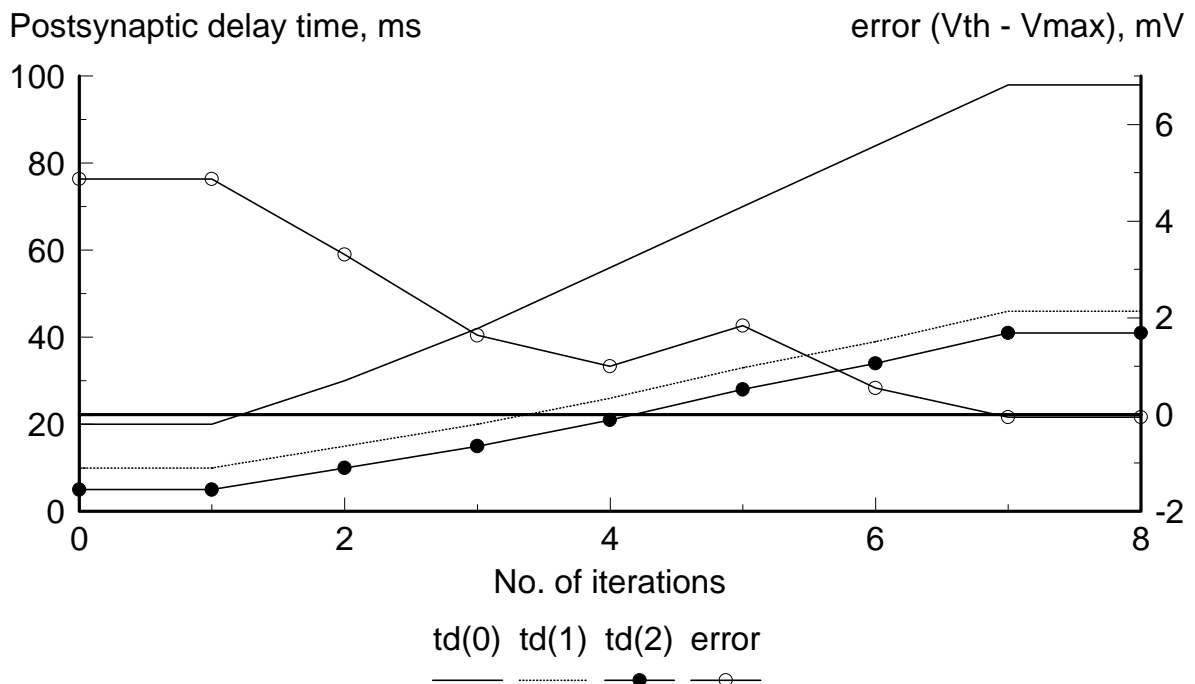

Figure 4: Postsynaptic delay modification and error adjustment during training. Learning rates: η = 0.3 and η' = 0.009. The final values of the delays are: $t_{d(0)}$ = 98ms, $t_{d(1)}$ = 46ms and $t_{d(2)}$ = 41ms.
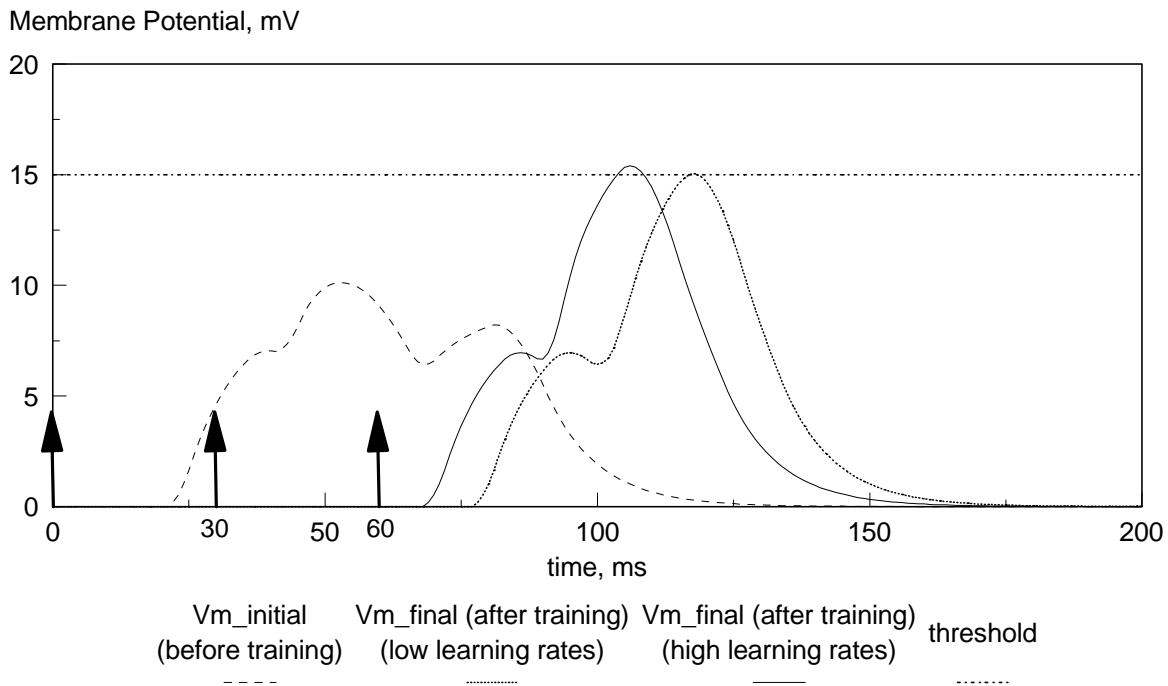
Membrane Potential, mV

Figure 5: Variation of the membrane potential before ($V_{m\_initial}$) and after training (V_{m_final}) for the two sets of learning rates, low: $\eta = 0.3$ and $\eta' = 0.009$ and high: $\eta = 0.5$ and $\eta' = 0.08$. When the membrane potential exceeds the threshold, the neuron fires and the temporal pattern is detected. The arrows indicate the time of arrival of each of the three spikes.

pattern after the seventh iteration. Certainly, the number of iterations required for the neuron to learn to detect a temporal pattern, depends on the learning rates. A simulation with higher learning rates of $\eta = 0.5$ and $\eta' = 0.08$ demonstrated that the detection of the temporal pattern could be achieved at the fourth iteration. Fig. 5 shows the variation of the membrane potential before and after training for low and high learning rates. It also indicates the time of arrival of each of the three spikes. As it can be seen, training increases the membrane potential with its maximum going above the threshold, enabling therefore the neuron to detect the temporal pattern presented.

5. Role of Stochastic Synapses (1-pRAMs) in the TNLI

Stochastic synapses can either generate EPSPs spontaneously or cause presynaptic spikes to fail to produce EPSPs. The first event is usually very infrequent, while transmission failures can occur with high probability. Both properties are mimicked by the 1-pRAMs used in the TNLI model. In the case of input spike trains with regularly spaced spikes, a stochastic synapse will cause the effective loss of some spikes and the appearance of spikes not part of the input spike train. Both effects result in EPSPs more irregularly spaced than the arriving spikes, thus increasing the effective Coefficient of Variation (C_V) (standard deviation/Mean Interspike Interval) (see Fig. 6). The stochastic transmission probability α_1 increases the C_V by decreasing the frequency of the regular spike train; the spontaneous probability α_0 increases the C_V by increasing the frequency of the input spike train and adds more noise causing the neuron to become more sensitive to small signals. In the case of bursting inputs, stochastic synapses will reduce the number of spikes in each burst and cause the appearance of spikes in inter-burst intervals. This decreases the effective C_V of the input spike train (see Fig. 6). In both cases
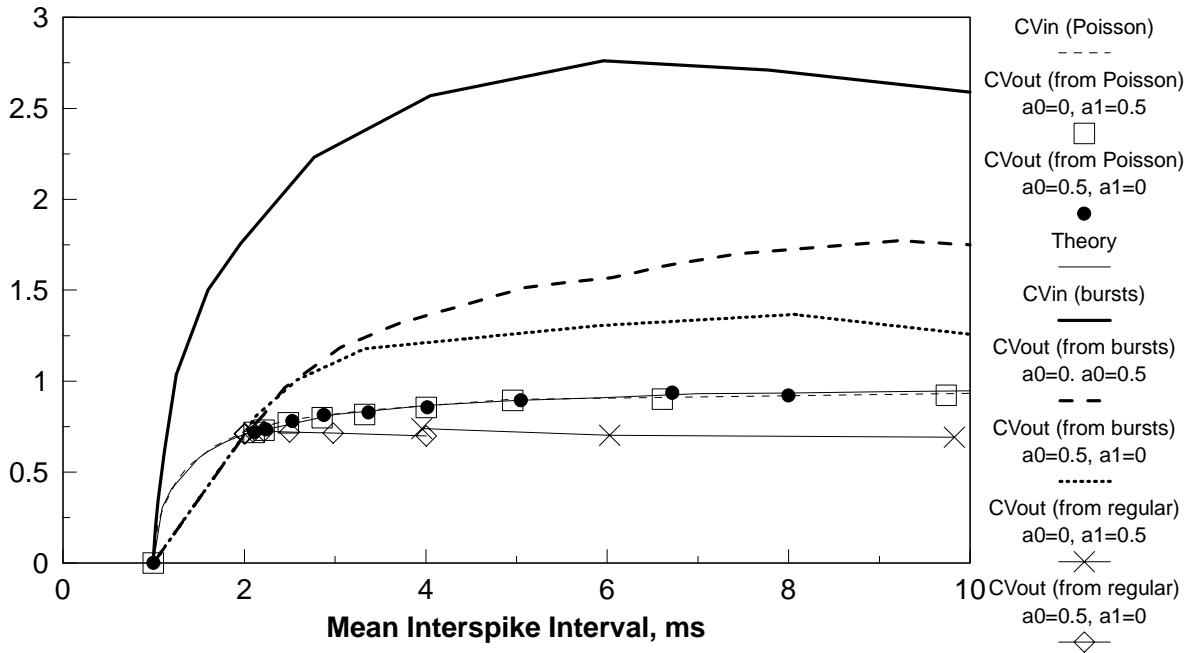
Cv (Coefficient of Variation)

Figure 6: Effect of 1-pRAMs for different configurations of the spontaneous (α_0) and stochastic (α_1) probabilities on Poisson ($C_V \simeq 1$), bursting ($C_V \gg 1$) and regular ($C_V = 0$) input spike trains. For all configurations the simulation was left to run for 10000ms. The full thin line (*theory*) shows the theoretical curve for a random spike train with discrete time steps given by: $C_V = \sqrt{(\Delta t_M - t_R) / \Delta t_M}$ (see Bugmann *et al.*, 1997).

stochastic synapses tend to bring the values of C_V closer to those of Poisson spike trains. When the inputs are already Poisson, stochastic synapses only alter the mean firing rate, generally reducing it, but they have a C_V staying on the theoretical C_V vs Δt_M (Mean Interspike Interval) curve (see Fig. 6).

Therefore the main role of stochastic synapses in the TNLI is to alter accordingly the variability of any spike train coming in, with proper adjustment of the probabilities of the 1-pRAMs. This adjustment can be achieved by employing local (synaptic) reinforcement learning (Clarkson *et al.*, 1992), whereby the reward/penalty signal will be based on the 0-pRAM probability value (input frequency) and also the C_V of the effective input spike train (i.e., the one after the 1-pRAMs).

6. Controlling the Variability of the Neuron's Firing using the TNLI

The control of the variability of firing in neurons and the determinants of this variability have attracted a huge interest after Softky & Koch (1993) demonstrated that the classical notion of a realistic neuron, i.e., being of a leaky integrator type, failed in reproducing the high variability they observed in cortical cells at high firing rates. Using the TNLI we examined the effect of inhibition on the firing variability (Christodoulou & Bugmann, 2000) in order to see whether it can be controlled. For the simulations we used random spike trains of controlled mean frequency (f_j) at the TNLI inputs, with $f_j = p/\Delta t$, where p is the 0-pRAM probability value. These random spike trains were unaffected by the 1-pRAM action in the current simulations. The 1-pRAMs were set to transmit perfectly each input spike since the inputs were already Poisson (see Section 5). f_j was the same for both excitatory and inhibitory inputs. Results were taken with 100 excitatory PSR generators and 0, 40, 80 and 95 inhibitory ones (denoting the number of
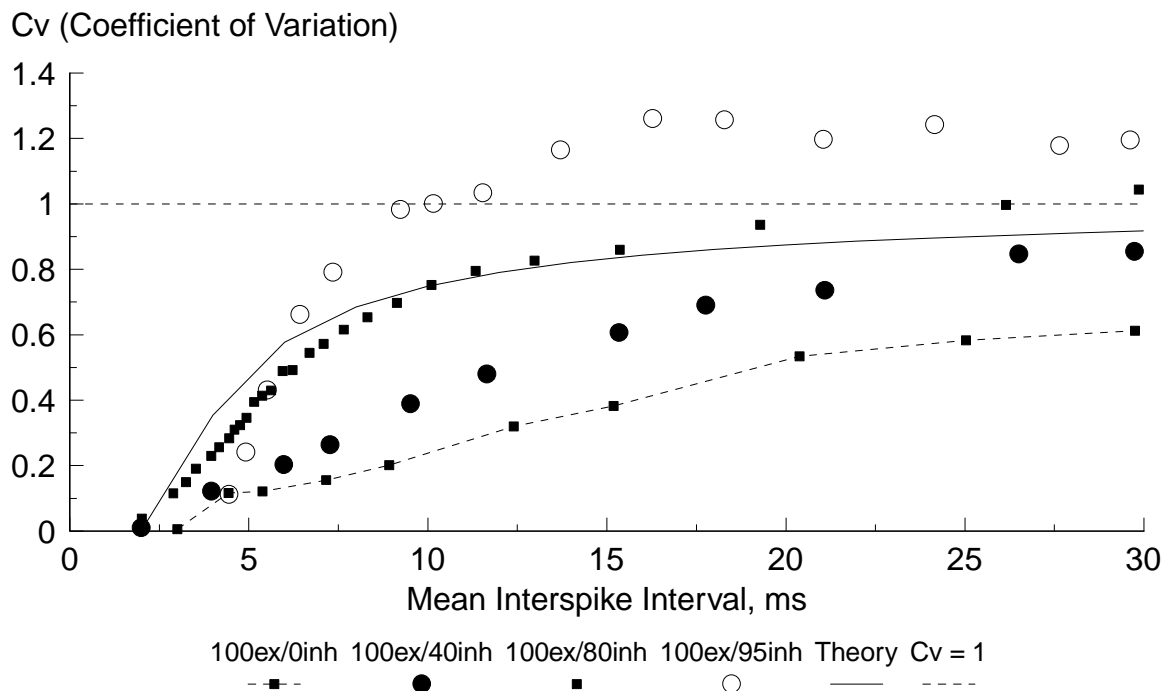
Figure 7: Coefficient of Variation (C_V) *vs* Mean Interspike Interval (Δt_M) showing the firing variability obtained with the TNLI neuron at different levels of inhibition. The C_V values with 80% inhibition are the closest to the ones observed experimentally. Simulation details: time step = 1ms; t_R (refractory period) = 2ms; V_{th} = 15mV; time constant = 10ms (R = 166MΩ, C = 60pF); parameter values used for the postsynaptic current responses (Fig. 1): t_d = 5ms, $d_r = d_f$ = 5ms, t_p = 10ms, h = 5pA. For simplicity, the inhibitory currents have an equal but opposite magnitude to the excitatory ones (-5pA). Full somatic reset was applied to the TNLI.

excitatory and inhibitory synaptic inputs). Fig. 7 shows the Coefficient of Variation (C_V) as a function of Δt_M, while the number of inhibitory inputs was increased. The full line shows the theoretical curve for a random spike train with discrete time steps (see caption of Fig. 6). If the simulated firing ISIs are Poissonian, then their C_V vs Δt_M curve should follow this theoretical curve. The C_V values obtained with 100 excitatory inputs and 80 inhibitory inputs (100ex/80inh, Fig. 7) are very similar to those observed in cortical neurons (see Fig. 9 in Softky & Koch, 1993). By looking also at the ISI histogram distributions for mean ISI Δt_M of 15ms (Fig. 8) for the different inhibition levels, we can see that with 80% inhibition when C_V = 0.870, the distribution follows a Poisson tail (exponential decay). The small initial hump at the beginning of the distribution is due to the presence of clusters of spikes at short intervals. This tendency to produce short clusters of spikes, is also revealed in the autocorrelogram of the firing ISIs (Christodoulou & Bugmann, 2001). Therefore, we can deduce that with 80% inhibition on concurrent excitation, near Poisson-type firing spike trains can be produced at high firing rates as observed in cortical neurons (Softky & Koch, 1993). The use of stochastic inputs also affects the high firing, near Poisson-type variability produced. Thus the TNLI can be used to control the firing variability of neurons.

7. Controlling the Gain of the Neuron using the TNLI
In this section we examine whether the inhibition mechanism in the TNLI can be used to control the gain of the neuron (Christodoulou *et al*., 2000). In the TNLI we only incorporate hyperpolarising inhibition with negative current pulses of controlled shape (IPSCs, Fig. 1), and not shunting inhibition. Such responses are produced by certain PSR generators which are
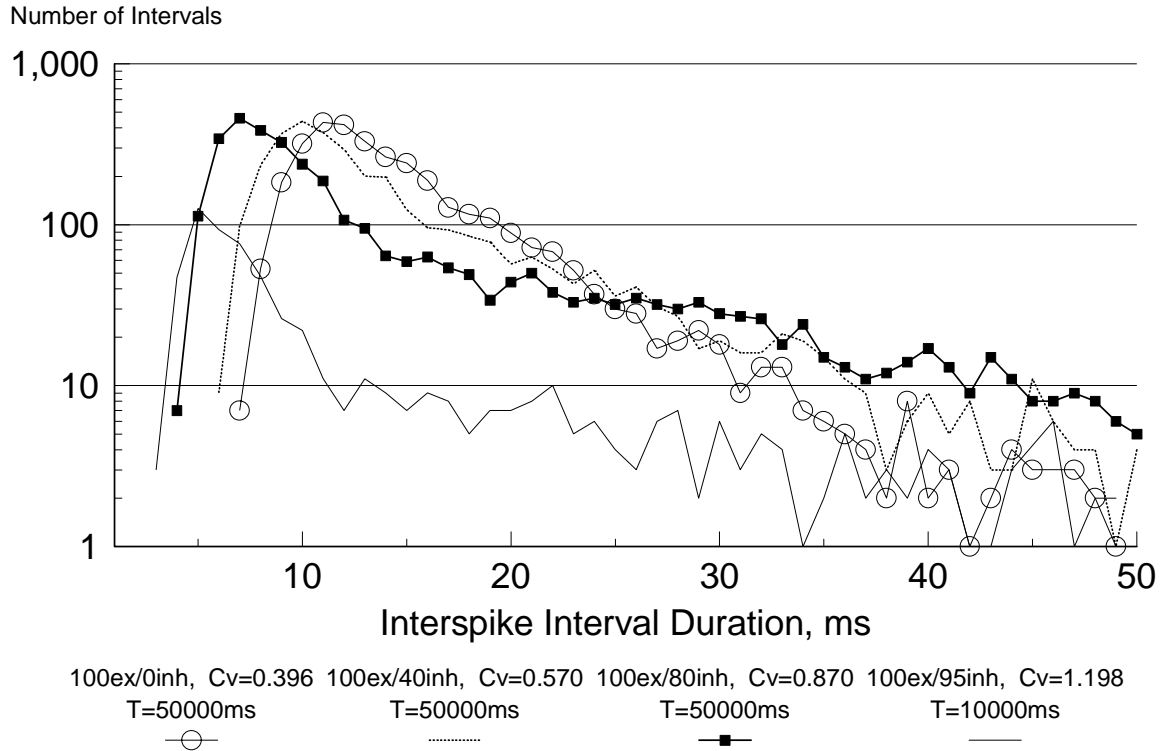
Number of Intervals

Figure 8: Interspike Interval histogram distributions for $\Delta t_M = 15$ms for different inhibition levels. *T* indicates the total time the system was left to operate. Rest of the parameter details as in Fig. 7.

assigned to be inhibitory ones. The number of inhibitory PSR generators which corresponds to inhibitory inputs is thus variable. In order to demonstrate the effects of inhibition, we vary this number and observe the change in the relationship between the Mean Input Current in neuron *i* (I_{M_i}) and the output frequency of the TNLI. I_{M_i} in the TNLI neuron *i* is given by:

$$I_{M_i} = \sum_{j=0}^{N} f_j \times PSR_{ij}^* \tag{11}$$

where f_j is the mean input spike frequency which in our simulations is the same for each input *j* and is given by the number of input spikes during time *T* (total time that the system is left to operate). *N* is the total number of input lines (or pRAMs). PSR_{ij}^* is the time integral of the postsynaptic current (PSR_{ij}) produced by a single spike arriving on input line *j* i.e.,

$$PSR_{ij}^* = \int_{0}^{d_r + t_p + d_f} PSR_{ij}(t)\ dt \tag{12}$$

Results were taken with 100 excitatory PSR generators and 0, 20, 40, 60, 80, 95 and 100 inhibitory ones (denoting the number of excitatory and inhibitory synaptic inputs). At the TNLI inputs, random spike trains of controlled mean frequency (f_j) were utilised (as in Section 6). While the number of inhibitory inputs was increased, we had to increase f_j, in order to obtain the same I_{M_i}. As indicated in Section 5, the frequency of the incoming spikes could have also been

increased intrinsically with the 1-pRAMs by increasing the spontaneous probability α_0. The output characteristic for the first six configurations above is shown in Fig. 9, where we also plotted the output frequency values of the balanced case of 100ex/100inh, in which case $I_{M_i} \simeq$ 0. In addition, Fig. 9 shows a plot of the excitatory component of I_{M_i} ($I_{M_{i_{ex}}}$) with the output firing frequency for the case of 100 excitatory and 40 inhibitory inputs. As it can be observed (Fig. 9) the TNLI gives a relatively steep sigmoidal nonlinear transfer function (esp. for low inhibition). This is due to the fact that for these simulations the somatic membrane potential is not reset after each spike (Bugmann *et al.*, 1997). The sigmoidal transfer function has a smooth and differentiable behaviour (positive derivative), which enables learning to be achieved using standard methods (Rumelhart *et al.*, 1986). This behaviour seems to be similar to that of the formal neuron (McCulloch & Pitts, 1943), which has a sigmoid transfer function given by: $y = 1/[1 + exp(-\gamma A_i)]$, where γ is a constant that determines the slope of the sigmoid and A_i is given by: $\sum x_j w_{ij}$ where x_j is the *jth* input to the neuron i and w_{ij} is the connection weight form neuron j to neuron i. A_i is equivalent to I_{M_i} in the TNLI (eqn. 11). Fig. 9 demonstrates that the introduction of the inhibition has the same effect as decreasing the value of γ in the sigmoid whereas in formal neurons inhibition only affects A_i. I_{M_i} is also modified when inhibition is introduced; the plot of $I_{M_{i_{ex}}}$ (excitatory component of I_{M_i}) with the output firing frequency for the case of 100 excitatory and 40 inhibitory inputs, shows that the sigmoid (and the threshold) is shifted horizontally toward higher $I_{M_{i_{ex}}}$ values which denotes that higher $I_{M_{i_{ex}}}$ is needed to obtain the same firing rate.

As it can be seen from Fig. 9 the slope of the sigmoid transfer function decreases as the strength of the introduced inhibition is increased. By looking at two snapshots of the membrane potential for $I_{M_i} = 80$pA and $I_{M_i} = 130$pA (vertical lines on Fig. 9), for the cases of 100ex/0inh,

100ex/0inh 100ex/20inh 100ex/40inh 100ex/60inh 100ex/80inh 100ex/95inh 100ex/40inh(Im_ex) 100ex/100inh
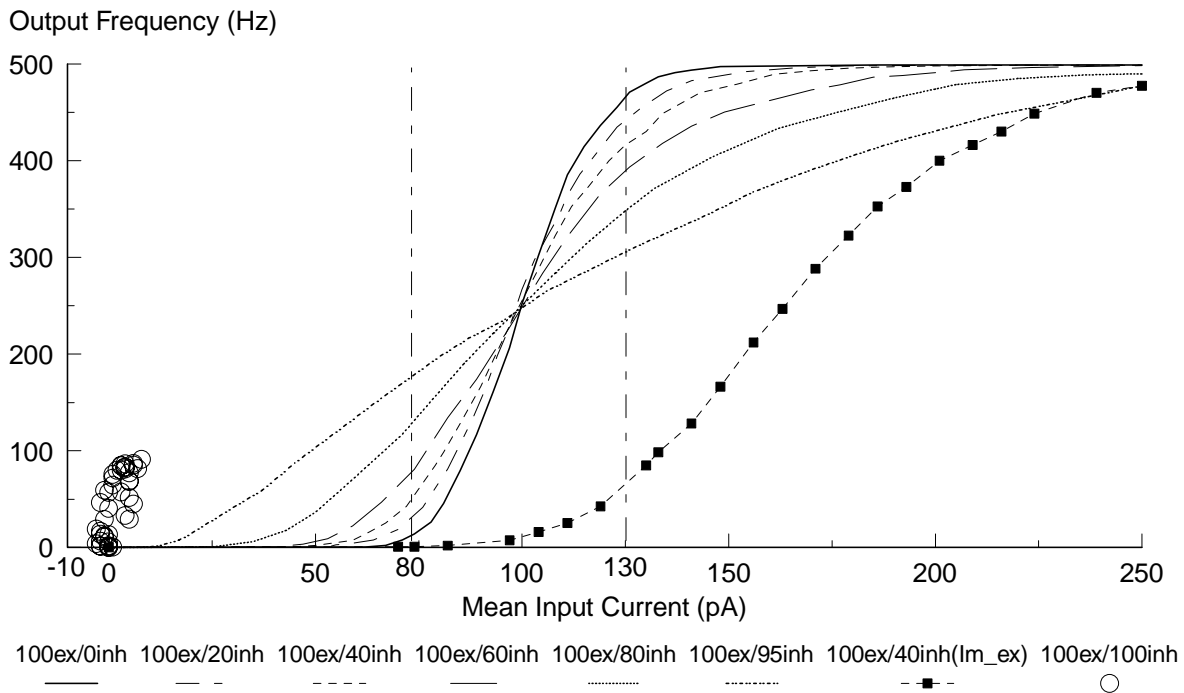
Figure 9: Transfer functions (TF) of the TNLI (Mean Input Current *vs* firing rate) with different levels of inhibition (see legends/text). TFs saturate at an output frequency of approx. 500Hz (which is equal to $1/t_R$). The simulation details are the same as the ones of Fig. 7. The total time that the system is left to operate is 10sec. No somatic reset was applied to the TNLI.

100ex/80inh and 100ex/95inh (shown in Fig. 10a, b from 0ms to 1000ms), it can be observed that inhibition increases frequency of the fluctuations of the membrane potential. It has to be noted that the increased fluctuations do not change the mean saturation level of the membrane potential. This is because of the higher excitatory input current which had to be induced when the number of inhibitory inputs was increased, in order to obtain the same mean input current I_{M_i} (see Fig. 9). In addition, the amplitude of the membrane potential fluctuations increases with inhibition as it can be seen from Fig. 10c, d, which show that the histogram distributions of the membrane potential widen with inhibition indicating that the membrane potential hits more times lower and higher amplitudes. Therefore, in the case of low I_{M_i} (e.g., 80pA, Fig. 10a), where the mean saturation level of the membrane potential is below the threshold, the membrane potential of the 100ex/80inh and the 100ex/95inh cases is able to exceed the threshold more frequently than in the 100ex/0inh case due to the greater amplitude fluctuations and thus give a higher output frequency. However, in the case of high I_{M_i} (e.g., 130pA, Fig. 10b) the mean saturation level of the membrane potential is above the threshold and so in the 100ex/80inh and the 100ex/95inh cases, due to the high amplitude fluctuations again, the membrane potential is able to go below the threshold more frequently than in the 100ex/0inh case and thus give a lower output frequency. This explains the reduced slope of the sigmoidal characteristic curves of Fig. 9 in the presence of inhibition. Alternatively, this can be also explained intuitively as follows: the total PSR at any given time is the sum of the excitatory and inhibitory PSRs occurring within
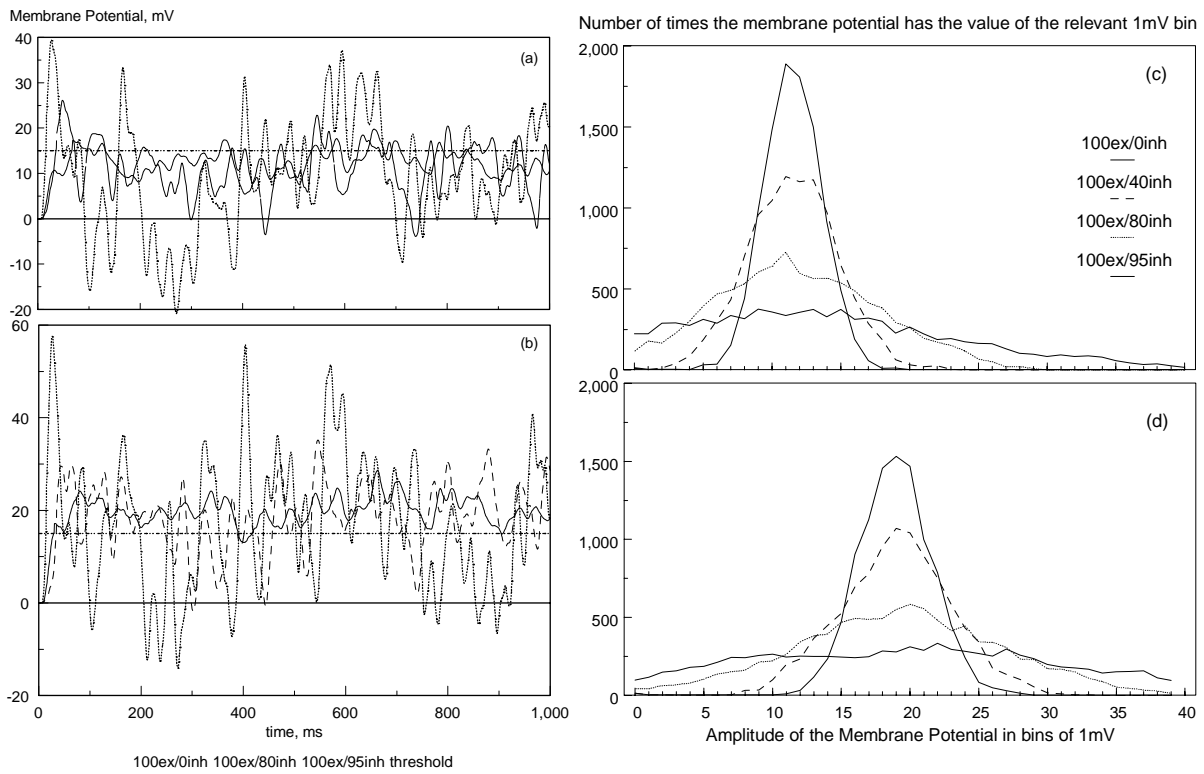

Figure 10: (a), **(b)** Membrane Potential without and with inhibition for the cases **100ex/0inh**, **100ex/80inh** and **100ex/95inh**) with the same Mean Input Current (I_{M_i}): (a) I_{M_i} = 80pA, (b) I_{M_i} = 130pA. Higher input frequencies are required to obtain the same I_{M_i} for the cases with inhibition. This results in a higher excitatory component of Mean Input Current which shifts the mean fluctuation level of the Membrane Potential above 0mV. **(c)**, **(d)** Histogram distributions of the Membrane Potential without inhibition and for three cases with inhibition (**100ex/0inh**, **100ex/40inh**, **100ex/80inh and 100ex/95inh**) with the same Mean Input Current (I_{M_i}): (c) I_{M_i} = 80pA, (d) I_{M_i} = 130pA.

a certain window. Thus the distribution of the total PSR will be the difference between the two binomial distributions (ignoring the ramped edges of the PSR). Adding more inhibition, requires more excitation to achieve the same mean. However, the variance of the distribution widens (as shown in Fig. 10c, d). When subtracting two independent distributions, the means subtract while the variances add. This point has previously been mentioned by Amit & Brunel (1997) (where they showed that spontaneous activity becomes self-stabilising in the presence of inhibition), but it has not been specifically proved by simulations as it is done here.

The other important point that can be deduced from Fig. 9 is that the decrease of the slope of the sigmoid output characteristic, which denotes the gain of the transfer function, seems to be proportional to the number of inhibitory inputs present. The gain is best reduced when the number of inhibitory inputs becomes nearly the same as the number of excitatory inputs (100ex/95inh case). Therefore, inhibition can be considered as another means of controlling the gain of the transfer function of the neuron. It has recently been demonstrated experimentally (Silberberg *et al*., 2000) that when the mean input current changes, it takes time for the firing rate to increase due to the integration time; when the variance of the input (the membrane potential in our case) increases however, the output firing rate reacts instantaneously. This indicates that our gain control mechanism, where we increase the variance of the membrane potential by increasing the input rate of inhibitory and excitatory postsynaptic currents, is an effective mechanism that real neurons can use. Other mechanisms of controlling the gain include: (i) total membrane conductance regulation via synaptic activity on descending pathways (Nelson, 1994) and (ii) partial somatic reset (Bugmann *et al*., 1997). The gain control mechanism by inhibition, is not shown or implied in the work of Amit and Brunel (1997).

When there is a balance of excitation and inhibition the mean input current is zero (see Fig. 9) and the neuron is firing due to the fluctuations. In this case, by looking at the relationship of the input frequency (f_j) and the firing rate of the neuron (not shown), we can deduce that in the case of balanced excitation and inhibition (where the neuron is explicitly firing due to the fluctuations), the firing rate can be controlled by the level of the mean input frequency.

8. Discussion

The TNLI spiking neuron model presented in this paper is an intermediate model between the fully biophysical multi-compartmental ones and formal neurons, which is simple enough to allow fast computations, while it maintains the observed stochastic and spatio-temporal characteristics of biological neural cells. The TNLI incorporates the important single neuron characteristics desirable in a model (see Section 1) namely: intrinsic stochasticity, nonlinearity and temporal sensitivity. The main differences of the TNLI from other models are: (i) the addition of the PSR generators which can add a variable time delay or change the shape of the postsynaptic currents, which may represent some computation by the dendrite (due to dendritic geometry or synaptic time delays), (ii) the modelling of the temporal summation of the PSRs and (iii) the ability to model stochastic synapses (represented by the 1-pRAMs). As we demonstrated in Section 5, in the case of bursting or regular input spike trains, the stochastic synapses tend to bring their variability closer to a Poisson one, while in the case of Poisson inputs, the variability stays the same. It has also been recently suggested (Senn *et al*., 2001b) that stochastic synapses might be important in the biological learning mechanism.

In Section 3, we demonstrated how the temporal power of the TNLI could be exploited. As it

was shown, the TNLI was successfully used as a motion and velocity detector system. The similarity of the velocity selectivity curve obtained with the TNLI to the one obtained experimentally in the H1 neuron of the visual system of the fly (Franceschini, 1985; Franceschini *et al.*, 1989) indicated that the TNLI has potential applications in artificial vision and could be incorporated in the vision system of the robot by Franceschini (Franceschini *et al.*, 1991; 1992), which was inspired by the visual system of the fly. The H1 neuron of the fly has also been modelled in analogue VLSI (Very Large Scale Integration) producing a neuromorphic motion sensor (Harrison & Koch, 1999) that simplified motor control by correcting to straight-line motion an imperfect motor path. Another interesting neuromorphic motion chip is the one used in the Koala robot (Indiveri & Douglas, 2000) which is modelled on the fly's wide-field direction selective cells. It remains to be seen how the digital realisation of the TNLI would compare with these analogue hardware models. It would also be interesting to explore the possibility of incorporating within a neuromorphic chip design the dendritic propagation delays which enabled the TNLI to model the velocity selectivity curve of the H1 cell. This technique complies with the latest findings that postsynaptic dendritic computation plays a significant role in the generation of directional selectivity by retinal ganglion cells (Taylor *et al*., 2000).

We have also demonstrated that a Hebbian-based learning rule can be used to train the postsynaptic delays of the TNLI neuron so that a temporal pattern can be detected and recognised, indicating the potential of the TNLI in dynamic time-dependent problems . The main target of the training is to achieve coincidence detection of the postsynaptic response currents so that the membrane potential is increased at a level above the threshold and enable thus the neuron to fire. The exact timing of the arriving spikes inducing postsynaptic responses is important in modifying the postsynaptic delays by using the learning rule to achieve coincidence detection, making thus the neuron sensitive to spike synchronisation. This approach, despite its simplicity, has similarities with the main idea of the experimental results by Markram *et al*. (1997). The achievement of coincidence detection was also the main aim in the training technique used in the biology-inspired pulse processing (BPN) neuron (Napp-Zinn, *et al*., 1996) which included delay adaptation, when applied for recognition and temporal tracking of discrete impulse patterns. These authors concluded that delay adaptation appeared to be a more effective mechanism for such applications, than weight adaptation. In addition, the use of Hebbian-type learning based on coincidence detection, was also suggested by Hopfield (Hopfield, 1994; 1995; 1996; Hopfield & Hertz, 1995) for the organised time delays which he uses to best represent time in his action potential model, which is an integrate-and-fire neuron model. Learning based on coincidence detection has also been studied by Gerstner *et al*. (1996; 1997).

In its present formulation, the learning rule has a result of producing spikes with long latencies, because it increases the latencies of EPSCs for achieving their overlap. For an effective integration of an animal with its environment, small latencies are more desirable. It must be noted that the learning process is a silent one, with spikes being produced only when the proper combination of synaptic delays has been achieved. Hence, once spikes are being produced, other mechanisms can come into play, such as spike backpropagation (Stuart & Sakmann, 1994; Frégnac, 1999; Larkum *et al*., 1999). It remains to be seen if these mechanisms could have the effect of reducing the latencies in subsequent learning epochs.

In Section 6, we demonstrated that the TNLI can be used to control the firing variability of neurons. This was achieved with concurrent excitation and inhibition (with inhibition being at

a level of 80% of excitation) and with random input spikes. The mechanism by which inhibition increases the firing variability is by introducing more short intervals in the firing pattern, resulting in near Poisson-type variability. The effect of concurrent inhibition and excitation was also examined by Feng & Brown (1998, 1999) who showed that the C_V is an increasing function of the length of the distribution of the input inter-arrival times and the degree of balance between excitation and inhibition (r). They also showed that there is a range of values of r that C_V values between 0.5 and 1 can be achieved (which is considered to be the physiological range) and this range excludes exact balancing between excitation and inhibition. The results of Feng & Brown do not answer to the problem posed by Softky & Koch (1993) for two reasons: (i) as they do not show a C_V *vs* Mean ISI curves, it is not clear whether the C_V values they obtained hold also for high firing rates and (ii) they only used the C_V statistic for assessing high variability which on its own is not a reliable indicator, since C_V values $\in$ [0.5, 1] are not equivalent with Poisson statistics. The effect of inhibition was also examined by Shadlen & Newsome (1994), who used a random walk model and by exact balancing of concurrent excitation and inhibition on a single cell, they produced highly irregular firing (compared to our results which suggest that only 80% inhibition to concurrent excitation is needed for producing highly irregular firing). The results of Shadlen & Newsome (1994) were disputed though by König et al. (1996) who questioned the biological realism of their assumptions, namely that there is an exact balance between excitatory and inhibitory inputs and the high rate of input signals. The assumption of how balanced excitation and inhibition is brought about naturally in model networks has also been studied by Amit & Brunel (1997) and Van Vreeswijk & Sompolinsky (1996; 1998). Shadlen & Newsome (1998) reiterate their previous findings by reinforcing both of their questionable assumptions with experimental evidence. It has to be noted that the above authors model both excitatory and inhibitory inputs as simple time series, which is different from the way we model them in the TNLI. This method of controlling the firing variability of a single neuron can be added to the two other methods previously reported namely: partial somatic reset (Bugmann *et al.*, 1997) and the use of temporally correlated inputs (Stevens & Zador, 1998).

In Section 7, we showed that the introduction of inhibition, not only reduces the mean input current for the same mean input frequency (shifting the transfer function), but it also decreases the slope of the transfer function (gain) of the neuron. The effect on the slope is due to increasing (i) the frequency of the fluctuations and (ii) the amplitude of the fluctuations of the membrane potential (at a given level of mean input current) around its mean saturation value. This goes beyond the assumption underlying the formal neuron used in Artificial Neural Networks where it is assumed that positive and negative inputs add linearly and then pass through a fixed sigmoidal transfer function, whereas in the TNLI the sigmoidal transfer function is modified by the signals passing through it. In other words, with inhibition, weak signals need less amplification to produce the same level of output frequency but strong signals need more amplification. In addition, it has been shown that inhibition can be used for controlling the gain of the transfer function of the neuron, with the gain being a decreasing function of the number of inhibitory inputs. Finally, in the case of balanced excitation and inhibition, when the neuron is totally driven by membrane potential fluctuations, the firing rate can be controlled by the level of the mean input frequency. Most of the authors who have examined the balance between excitation and inhibition (Shadlen & Newsome, 1994; 1998; Feng & Brown 1998; Tsodyks & Sejnowski, 1995; Van Vreeswiijk & Sompolinsky, 1996; 1998), have not explored how the firing rate can be controlled in such a case, apart from Nelson (1994) who uses a slightly different method. In particular, Nelson's (1994) method uses activity levels (i.e., input frequencies) of

inhibitory and excitatory inputs, which are descending inputs from higher brain centres that regulate the cell's membrane conductance and the ascending sensory input is not controlled directly. Such a mechanism appears highly plausible in the electrosensory system of an electric fish. Nelson (1994) showed that the adjustment of the input frequencies induces a change in the membrane conductance which leads to gain regulation.

In summary we conclude through the applications shown as examples in this paper, that the TNLI despite its simplicity can be used in both (i) dynamic applications like motion detection and temporal pattern recognition in general, based on postsynaptic delay training and (ii) in applications in Computational Neuroscience where it can give us insight on certain phenomena that are not easily revealed by experimental studies as well as capturing in artificial systems the dynamics of biological neural mechanisms.

References
Abbott, L. F. and Kepler, T. B. (1990). Model neurons: from Hodgkin Huxley to Hopfield. In: *Statistical Mechanics of Neural Networks*, ed. by Garrido, L., Lecture Notes in Physics, **368**, Springer, Berlin, 5-18.

Amit, D. J. & Brunel, N. (1997). Global spontaneous activity and local structured (learned) delay activity in cortex. *Cerebral Cortex*, **7**, 237-252.

Bernander, Ö., Douglas, R. J., Martin, K. A. C. & Koch, C. (1991). Synaptic background activity influences spatiotemporal integration in single pyramidal cells. *Proc. Natl. Acad. Sci. USA*, **88**, 11569-11573.

Bialek, W., Rieke, F., Vansteveninck, R. R. D. & Warland, D. (1991). Reading a neural code. *Science*, **252**, 1854-1857.

Borst, A. & Egelhaaf, M. (1995). Visuomotor coordination in flies. In: *The handbook of brain theory and neural networks*, ed. by Arbib, M. A., MIT Press, USA, 1031-1036.

Bressloff, P. C. & Taylor, J. G. (1991). Discrete Time Leaky Integrator Network with Synaptic Noise. *Neural Networks*, **4**, 789-801.

Bressloff, P. C. & Taylor, J. G. (1993). Spatiotemporal pattern processing in a compartmental-model neuron. *Physical Review E*, **47**, 4, 2899-2912.

Buchmann, J., & Schulten, K. (1987). Influence of noise on the function of a "Physiological" neural network. *Biol. Cybern.*, **56**, 313-327.

Buchner, E. (1976). Elementary movement detectors in an insect visual system. *Biol. Cybern.*, **24**, 85-101.

Buchner, E. (1984). Behavioural analysis of spatial vision in insects. In: *Photoreception and vision in invertebrates*, ed. by Ali, M. A., Plenum, New York, 561-621.

Bugmann, G. (1992). Multiplying with neurons: Compensation for irregular input spike trains by using time-dependent synaptic efficiencies. *Biol. Cybern.*, **68**, 87-92.

Bugmann, G., Christodoulou C. & Taylor, J. G. (1997). Role of temporal integration and fluctuation detection in the highly irregular firing of a Leaky Integrator neuron with partial reset. *Neural Computation*, **9**, 5, 985-1000.

Burgi, P. Y. & Pun, T. (1991). Figure-ground separation: evidence for asynchronous processing in visual perception?. *Perception*, **20**, 69.

Burke, R. E. & Rudomin, P. (1977). Spinal neurons and synapses. *Handbook of Physiology*, *The nervous system*, Section 1, Vol. 1, Part 2, Ch. 24, (ed. E. R. Kandel), American Physiological Society, Bethesda, Maryland, USA, 877-944.

Bush, P. & Douglas, R. J. (1991). Synchronisation of bursting action potential discharge. *Neural Computation*, **3**, 19-30.

Butz, E. G. & Cowan, J. D. (1974). Transient potentials in dendritic systems of arbitrary geometry. *Biophys. J.*, **14**, 661-689.

Christodoulou, C., Bugmann, G., Taylor, J. G. & Clarkson, T. G. (1992). An extension of the Temporal Noisy-Leaky Integrator neuron and its potential applications. *Proc. of the Int. Joint Conf. on Neural Networks*, Beijing, **III**, 165-170.

Christodoulou, C., Clarkson T. G. & Taylor, J. G. (1995). Temporal pattern detection and recognition using the Temporal Noisy-Leaky Integrator neuron model with the postsynaptic delays trained using Hebbian Learning. *Proc. of the World Congress on Neural Networks (WCNN'95)*, Washington, DC, USA, **Vol. 3**, 34-37.

Christodoulou, C. & Bugmann, G. (2000). Near-Poisson-Type Firing Produced by Concurrent Excitation and Inhibition. *Biosystems*, **58**, 41-48.

Christodoulou, C., Clarkson, T.G., Bugmann, G. & Taylor, J.G. (2000). Analysis of Fluctuation-Induced firing in the presence of inhibition. *Proc. Int Joint Conf on Neural Networks 2000*, Como, Italy, IEEE Computer Society Press, Vol. III, 115-120.

Christodoulou, C. & Bugmann, G. (2001). Coefficient of Variation (CV) vs Mean Interspike Interval (ISI) curves: what do they tell us about the brain? *Neurocomputing*, **38-40**, 1141-1149.

Clarkson, T. G., Ng, C. K., Gorse, D & Taylor, J. G. (1992). Learning Probabilistic RAM Nets using VLSI structures. *IEEE Trans. on Computers*, **41** (12), 1552-1561.

Clarkson, T. G., Ng, C. K. & Guan, Y. (1993). The pRAM: An adaptive VLSI chip. *IEEE Trans. on Neural Networks*, **4** (3), 408-412.

Cronin, J. (1987). *Mathematical aspects of Hodgkin-Huxley neural theory*. Cambridge University Press, Cambridge, UK.

Davis, L., Jr. & Lorente de Nó, R. (1947). Contribution to the mathematical theory of the electrotonus. *Studies from the Rockefeller Institute for Medical Research*. **131**, 442-496.

Ekeberg, Ö, Wallen, P., Lanser, A. Traven, H., Brodin, L. & Grillner, S. (1991). A computer-based model for realistic simulations of neural networks. *Biol. Cybern.*, **65**, 81-90.

Feng, J. & Brown, D. (1998). Impact of temporal variation and the balance between excitation and inhibition on the output of the perfect integrate-and-fire model. *Biol. Cybern.*, **78**, 369-376.

Feng, J. & Brown, D. (1999). Coefficient of Variation of interspike intervals greater than 0.5. How and when? *Biol. Cybern.*, **80**, 291-297.

FitzHugh, R. (1961). Impulses and physiological states in theoretical models of nerve membranes. *Biophys. J.*, **65**, 81-90.

Franceschini, N. (1985). Early processing of colour and motion in a mosaic visual system. *Neuroscience Research*, Suppl. 2, Elsevier, Ireland, S17-S49.

Franceschini, N., Riehle, A. & Le Nestur, A. (1989). Directionally selective motion detection by insect neurons. In: *Facets of vision*, ed. by Stavenga, D. G. and Hardie, R. C., Springer-Verlag, Berlin, Heidelberg, Ch. 17, 360-390.

Franceschini, N., Pichon, J-M. & Blanes, C. (1991). Real time visuomotor control: from flies to robots. *Proc. 5th IEEE Int. Conf. on Adv. Robotics*, Pisa, Italy, 931-935.

Franceschini, N., Pichon, J. M. & Blanes, C. (1992). From insect vision to robot vision. *Philos. Trans. R. Soc. Lond. B, Biol. Sci.*, **337**, 283-294.

Frégnac, Y. (1999). A tale of two spikes. *Nature Neuroscience*, **2**, 299-301.

Fusi, S., Annunziato,, M., Badoni, D., Salamon, A., Amit, D. J. (2000). Spike-driven synaptic plasticity: theory, simulation, VLSI implementation. *Neural Computation*, **12**, 2227-2258.

Gerstner, W. (1998). Spiking Neurons. In W. Maass & C. M. Bishop (Eds.) *Pulsed Neural Networks* (pp. 261-295). Cambridge: MIT Press.

Gerstner, W., Kempter, R., van Hemmen, J. L. and Wagner, H. (1997). A developmental learning rule for coincidence tuning in the barn owl auditory system. In: *Computational Neuroscience: Trends in Research 1997*, Plenum Press: New York, 665-669.

Gerstner, W., Kempter, R., van Hemmen, J. L., & Wagner, H. (1996). A neuronal learning rule for

sub-millisecond temporal coding. *Nature*, **383**,76-78

Hassenstein, B. & Reichardt, W. (1956). Systemtheoretische Analyse der Zeit-, Reinfolgen- und Vorzeichenauswertung bei der Bewegungsperzeption des Rüsselkäfers *Chlorofaphanus*. *Z. Naturforsch*, **11b**, 513-524.

Harrison, R. R. & Koch, C. (1999). A robust analogue VLSI motion sensor based on the visual system of the fly. *Autonomous Robots*, **7**, 211-224.

Hausen, K. & Egelhaaf, M. (1989). Ch. 18: Neural mechanisms of visual course control in insects. In: *Facets of Vision*, ed. by D. G. Stavenga & R. C. Hardie, Springer, Berlin, 391-424.

Hebb, D. O. (1949). *The Organisation of Behaviour: A Neurophysiological Theory*, New York: Wiley.

Hodgkin, A. L. & Rushton, W. A. H. (1946). The electrical constants of a crustacean nerve fibre. *Proc. Roy. Soc. London B*. **133**, 444-479.

Hodgkin, A. L. & Huxley, A F. (1952). A quantitative description of membrane current and its application to conduction and excitation in a nerve. *J. of Physiol.* (London), **117**, 500-544.

Holmes, W. R. (1986). A continuous cable method for determining the transient potential in passive trees of known geometry. *Biol. Cybern.*, **55**, 115-124.

Hopfield, J. J. (1984). Neurons with graded response have collective computational properties like those of two-state neurons. *Proc. Natl. Acad. Sci.,* USA, **81**, 3088-3092.

Hopfield, J. J. (1994). Neurons, Dynamics and Computation. *Physics Today*, February 1994, 40-46.

Hopfield, J. J. (1995). Pattern recognition computation using action potential timing for stimulus representation. *Nature*, **376**, 33-36.

Hopfield, J. J. (1996). Transforming neural computations and representing time. *Proc. Natl. Acad. Sci.,* USA, **93**, 15440-15444.

Hopfield, J. J. & Hertz, A. V. M. (1995). Rapid local synchronisation of action potentials: Toward computation with coupled integrate-and-fire neurons. *Proc. Natl. Acad. Sci. USA*, **92**, 6655-6662.

Horwitz, B. (1981). An analytical method for investigating transient potentials in neurons with branching dendritic trees. *Biophys. J.*, **36**, 155-192.

Horwitz, B. (1983). Unequal diameters and their effect on time-varying voltages in branched neuron. *Biophys. J.*, **41**, 51-66.

Indiveri, G. & Douglas, R. (2000). Neuromorphic Vision Sensors. *Science*, **288**, 1189-1190.

Jack, J. J. B., Noble, D. and Tsien, R. W. (1975). *Electric current flow in excitable cells*. Oxford University Press.

Katz, B. (1969). *The release of Neural Transmitter substance*. Liverpool University Press, Liverpool.

Kempter, R., Gerstner, W., & van Hemmen, J. L. (1999). Hebbian Learning and Spiking Neurons. *Physical Review E*, **59**, 4498-4514.

Kistler, W. M. & van Hemmen, J. L. (2000). Modelling Synaptic Plasticity in Conjunction with the Timing of Pre- and Postsynaptic Action Potentials. *Neural Computation*, **12**, 385-405.

Kitajima, T. & Hara, K. (2000). A generalised Hebbian rule for activity-dependent synaptic modifications. *Neural Networks*, **13**, 445-454.

Koch, C., Poggio, T. & Torre, V. (1982). Retinal ganglion cells: a functional interpretation of dendritic morphology. *Phil, Trans. R. Soc. London (Biol.)*, **298**, 227-264.

Koch, C. & Poggio, T. (1985). A simple algorithm for solving the cable equation in dendritic trees of arbitrary geometry. *J. Neurosci. Meth.*, **12**, 303-315.

Koch, C., Poggio, T. & Torre, V. (1986). Computations in the vertebrate retina: gain enhancement, differentiation and motion discrimination. *Trends in Neurosciences*, **9**, 5, 204-211.

Koch, C. & Mathur, B. (1996). Neuromorphic vision chips. *IEEE Spectrum*, May 1996, 38-46.

Koch, C. and Segev, I. (eds) (1998). *Methods in Neuronal Modelling*. (2nd. ed.). MIT Press, Cambridge, MA.

Kohonen, T. (1988). *Self-organisation and associative memory*, 2nd ed., Springer-Verlag.

König, P., Engel, A. K. & Singer, W. (1996). Integrator or Coincidence Detector? The role of the cortical neuron revisited. *Trends in Neurosciences*, **19**, 130-137.

Larkum, M. E., Zhu, J. J. & Sakmann, B. (1999). A new cellular mechanism for coupling inputs arriving

at different cortical layers. *Nature*, **398**, 338-341.

Lapique, L. (1907). Reserches quantatives sur l' excitation électrique des nerfs traitée comme une polarization. *J. Physiol. Pathol. Gen.,* **9**, 620-635.

Levick, W. R. & Zacks, J. L. (1970). Responses of cat ganglion cells to brief flashes of light. *J. Physiol.*, **206**, 677-700.

Maass, W. (2001). Computation with spiking neurons. In: M. A. Arbib, editor, *The Handbook of Brain Theory and Neural Networks*. MIT Press (Cambridge), 2nd edition (to appear in November 2002, ISBN 0262011972).

Markram, H., Lübke, J., Frotscher, M & Sakmann B. (1997). Regulation of Synaptic Efficacy by Coincidence of Postsynaptic APs and EPSPs. *Science*, **275**, 213-215.

McCulloch, W. S. & Pitts, W. (1943). A logical calculus of the ideas immanent in nervous activity. *Bull. Math. Biophys.*, **5**, 115-133.

Nagumo, J. S., Arimoto, S. and Yoshizawa, S. (1962). An active pulse transmission line simulating nerve axon. *Proc. IRE*, **50**, 2061-2070.

Napp-Zinn, H., Jansen, M. & Eckmiller, R. (1996). Recognition and Tracking of impulse patterns with delay adaptation in biology-inspired pulse processing neural net (BPN) hardware. *Biol. Cybern.*, **74**, 449-453.

Nelson, M. E. (1994). A mechanism for neuronal gain control by descending pathways. *Neural Computation*, **6**, 242-254.

Nicholls, J. G., Martin, A. R. & B. G. Wallace, B. G. (1992). *From Neuron to Brain: A Cellular and Molecular Approach to the Function of the Nervous System*, Sunderland, MA, USA, Sinauer Associates.

Poggio, T. & Torre, V. (1977). A new approach to synaptic interactions. In: *Lecture notes in Biomathematics. Theoretical Approaches to Computer Systems, Vol. 21.* Ed. by Heim, H. and Palm, G., Springer, Berlin, 89-115.

Pun, R. Y. K., Neale, E. A., Cuthrie, P. B. & Nelson, P. G. (1986). Active and Inactive Central Synapses in the Cell Culture. *J. of Neurophysiol.,* **56**, (5), 1242-1256.

Rall, W. (1959). Branching dendritic trees and motoneuron membrane resistivity. *Exp. Neurol.*, **2**, 503-532.

Rall, W. (1962). Theory of physiological properties of dendrites. *Ann. N. Y. Acad. Sci.*, **96**, 1071-1092.

Rall, W. (1964). Theoretical significance of dendritic trees for neuronal input-output relations. *In: Neural Theory and Modelling.* Ed. by Reiss,. R. F., Stanford, Stanford University Press, 73-77.

Rall, W. (1977). Core conductor theory and cable properties of neurons. In: *Handbook of Physiology: The Nervous System, Vol. 1*, ed. by Kandel, E. R., Brookhardt, J. M. and Mountcastle, V. B., Williams and Williams, Co., Baltimore, Maryland, USA, 39-98.

Rall, W. & Agmon-Snir, H. (1998). Cable theory for dendritic neurons. In: *Methods in Neuronal Modelling: From Ions to Networks* (2nd ed), ed. by C. Koch & I. Segev, Ch. 2, 27-92, Cambridge, MA: MIT Press.

Rapp, M., Yarom, Y. & Segev, I. (1992). The impact of parallel fiber background activity on the cable properties of cerebellar Purkinje cells. *Neural Computation*, **4**, 518-533.

Redman, S. (1986). Monosynaptic transmission in the spinal cord. *News in Physiol. Sci.* **1**, 171-174.

Redman, S. (1990). Quantal analysis of synaptic potentials in neurons of the central nervous system. *Physiol. Rev.*, **70**, 165-198.

Reichardt, W. (1961). Autocorrelation: A principle for the evaluation of sensory information by the central nervous system. In: *Sensory Communication*, ed. by W. A. Rosenblith, MIT Press/Wiley, NY, USA, 303-317.

Reichardt, W. (1987). Evaluation of optical motion information by movement detectors. *J. Comp. Physiol. [A]*, **161**, 533-547.

Reiss, M. & Taylor, J. G. (1991). Storing temporal sequences. *Neural Networks*, **4**, 773-787.

Rieke, F., Warland, D., de Ruyter van Steveninck & Bialek, W. (1997). *Spikes: Exploring the neural code*, Cambridge, MA, MIT.

Rinzel, J. & Rall, W. (1974). Transient response in a dendritic neuron model for current injected at one

branch. *Biophys. J.*, **14**, 759-790.

Rinzel, J. & Ermentrout, B. (1998). Analysis of Neural Excitability and Oscillations. In: *Methods in Neuronal Modelling: From Ions to Networks* (2nd ed), ed. by C. Koch & I. Segev, Ch.7, 251-292.

Rumelhart, D. E., Hinton, G. E. and Williams, R. J. (1986). Learning representations by back-propagating errors. *Nature*, **323**, 533-536.

Segev, I. & Burke, R. E. (1998). Compartmental Models of Complex Neurons. In: *Methods in Neuronal Modelling: From Ions to Networks* (2nd ed), ed. by C. Koch & I. Segev, Ch.3, 93-136.

Senn, W., Markram, H. & Tsodyks, M. (2001a). An algorithm for modifying neurotransmitter release probability based on pre- and post-synaptic spike timing. *Neural Computation*,**13** 35-67.

Senn, W., Schneider, M. & Ruf, B. (2001b). Activity-dependent selection of axonal and dendritic delays, or, why synaptic transmission should be unreliable. *Neural Computation*, **14**, 583-619.

Shadlen, M. N. & Newsome, W. T. (1994). Noise, neural codes and cortical organisation *Curr. Opin. Neurobiol.*, **4**, 569-579.

Shadlen, M. N. & Newsome, W. T. (1998). The variable discharge of cortical neurons: Implications for connectivity, computation, and information coding. *J of Neurosci.*, **18**, 3870-3896.

Silberberg, G., Tsodyks, M., Markram, H. (2000). Differential impact on neuronal discharge of changing mean current vs current noise. *Eur. J. Neurosci.* **12**, Suppl. S 502-502.

Softky, W. R. & Koch, C. (1993). The Highly Irregular Firing of Cortical Cells Is Inconsistent with Temporal Integration of Random EPSP's. *J. of Neurosci.*, **13** (1), 334-530.

Song, S., Miller, K. D. & Abbot, L. F. (2000). Competitive Hebbian Learning through Spike-Timing dependent synaptic plasticity. *Nature Neuroscience*, **3**, 919-926.

Srinivasan, M. V., Poteser, M. & Kral, K. (1999). Motion detection in insect orientation and navigation. *Vision Research*, **39**, 2749-2766.

Stein, R. B. (1967). The frequency of nerve action potential generated by applied currents. *Proc. R. Soc. London, B*, **167**, 64-86.

Stevens, C. F. & Zador, A. M. (1998). Input synchrony and the irregular firing of cortical neurons. *Nature Neurosci.* **1**, 210-217.

Stuart, G. J. & Sakmann, B. (1994). Active propagation of somatic action potentials into neocortical pyramidal cell dendrites. *Nature*, **367**, 69-72.

Taylor, J. G. (1972). Spontaneous behaviour in Neural Networks. *J. of Theor. Biol.*, **36**, 513-528.

Taylor, W. R., He, S. Levick, W. R. & Vaney, D. I. (2000). Dendritic Computation of Direction Selectivity by Retinal Ganglion Cells. *Science*, **289**, 2347-2350.

Tsodyks, M. V. & Sejnowski, T. (1995). Rapid state switching in balanced cortical network models. *Network: Computation in Neural Systems*, **6**, 111-124.

Tuckwell, H. C. (1988). *Introduction to theoretical neurobiology: volume 1, Linear cable theory and dendritic structure.* Cambridge University Press, Cambridge, UK.

Van Vreeswijk, C. & Sompolinsky, H. (1996). Chaos in neuronal networks with balanced excitatory and inhibitory activity. *Science*, **274**, 1724-1726.

Van Vreeswijk, C. & Sompolinsky, H. (1998). Chaotic balanced state in a model of cortical circuits. *Neural Comput.*, **10**, 1321-1371.

Walmsley, B. & Stuklis, R. (1989). Effects of spatial and temporal dispersion of synaptic input on the time course of synaptic potentials. *J. of Neurophysiol.*, **61**, 681-687.

Wilson, C. J. (1984). Passive cable properties of dendritic spines and spiny neurons. *J. Neurosci.*, **4**, 281-297.

Zanker, J. M., Srinivasan, M. V. & Egelhaaf, M. (1999). Speed tuning in elementary motion detectors of the correlation type. *Biol. Cybern.*, **80**, 109-116.